

1 **Antigenicity and Immunogenicity of Differentially Glycosylated HCV E2**

2 **Envelope Proteins Expressed in Mammalian and Insect Cells**

3

4 Richard A. Urbanowicz^{1,2*}, Ruixue Wang^{3,4*}, John E. Schiel⁵, Zhen-yong Keck⁶, Melissa C.

5 Kerzic^{3,4}, Patrick Lau⁶, Sneha Rangarajan^{3,4}, Kyle J. Garagusi^{3,4}, Lei Tan⁶, Johnathan D.

6 Guest^{3,4}, Jonathan K. Ball^{1,2}, Brian G. Pierce^{3,4}, Roy A. Mariuzza^{3,4}, Steven K. H. Fong⁶,

7 and Thomas R. Fuerst^{3,4#}

8

9 ¹School of Life Sciences, The University of Nottingham, Nottingham, NG7 2RD UK, ²NIHR

10 Nottingham Biomedical Research Centre, Nottingham University Hospitals NHS Trust and

11 The University of Nottingham, Nottingham, NG7 2UH UK, ³University of Maryland

12 Institute for Bioscience and Biotechnology Research, W. M. Keck Laboratory for Structural

13 Biology, Rockville, MD 20850, ⁴Department of Cell Biology and Molecular Genetics,

14 University of Maryland, College Park, Maryland 20742, ⁵University of Maryland Institute for

15 Bioscience and Biotechnology Research, National Institute of Standards and Technology,

16 Rockville, MD 20850, ⁶Department of Pathology, Stanford University School of Medicine,

17 Stanford, California 94304

18

19 Running head: Immunogenicity of Differentially Glycosylated HCV E2

20 #Address correspondence to Thomas R. Fuerst, tfuerst@umd.edu

21 *R.U. and R.W. contributed equally to this manuscript.

22 Word count abstract: 248 words, text: 6,679 words

23 **ABSTRACT**

24 Development of a prophylactic vaccine for hepatitis C virus (HCV) remains a global health
25 challenge. Cumulative evidence supports the importance of antibodies targeting the HCV E2
26 envelope glycoprotein to facilitate viral clearance. However, a significant challenge for a B
27 cell-based vaccine is focusing the immune response on conserved E2 epitopes capable of
28 eliciting neutralizing antibodies not associated with viral escape. We hypothesized that
29 glycosylation might influence the antigenicity and immunogenicity of E2. Accordingly, we
30 performed head-to-head molecular, antigenic and immunogenic comparisons of soluble E2
31 (sE2) produced in (i) mammalian (HEK293) cells, which confer mostly complex and high
32 mannose type glycans; and (ii) insect (Sf9) cells, which impart mainly paucimannose type
33 glycans. Mass spectrometry demonstrated that all 11 predicted N-glycosylation sites were
34 utilized in both HEK293- and Sf9-derived sE2, but that N-glycans in insect sE2 were on
35 average smaller and less complex. Both proteins bound CD81 and were recognized by
36 conformation-dependent antibodies. Mouse immunogenicity studies revealed that similar
37 polyclonal antibody responses were generated against antigenic domains A–E of E2.
38 Although neutralizing antibody titers showed that Sf9-derived sE2 induced moderately
39 stronger responses than HEK293-derived sE2 against the homologous HCV H77c isolate,
40 the two proteins elicited comparable neutralization titers against heterologous isolates. Given
41 that global alteration of HCV E2 glycosylation by expression in different hosts did not
42 appreciably affect antigenicity or overall immunogenicity, a more productive approach to
43 increasing the antibody response to neutralizing epitopes may be complete deletion, rather
44 than just modification, of specific N-glycans proximal to these epitopes.

45 **IMPORTANCE**

46 Development of a vaccine for hepatitis C virus (HCV) remains a global health
47 challenge. A major challenge for vaccine development is focusing the immune response on
48 conserved regions of the HCV envelope protein, E2, capable of eliciting neutralizing
49 antibodies. Modification of E2 by glycosylation might influence the immunogenicity of E2.
50 Accordingly, we performed molecular and immunogenic comparisons of E2 produced in
51 mammalian and insect cells. Mass spectrometry demonstrated that the predicted
52 glycosylation sites were utilized in both mammalian and insect cell E2, although the glycan
53 types in insect cell E2 were smaller and less complex. Mouse immunogenicity studies
54 revealed similar polyclonal antibody responses. However, insect cell E2 induced stronger
55 neutralizing antibody responses against the homologous isolate used in the vaccine, albeit
56 the two proteins elicited comparable neutralization titers against heterologous isolates. A
57 more productive approach for vaccine development may be complete deletion of specific
58 glycans in the E2 protein.

59

60 **INTRODUCTION**

61 Hepatitis C virus (HCV) is a major public health problem and infects over 71 million
62 people worldwide (1). Infection often develops into chronic hepatitis, which is the most
63 prevalent cause of liver failure and hepatocellular carcinoma. In recent years, new direct
64 acting antivirals (DAAs) have supplanted the use of ribavirin and pegylated interferon alpha
65 as a treatment regimen, reaching cures rates of greater than 90% in HCV genotype 1-infected
66 patients (2, 3). However, significant limitations still exist, including the high cost of DAAs

67 that restricts access in developing countries where the disease burden is greatest (3) and
68 concerns about the development of drug resistance (2, 3). Moreover, therapy-induced HCV
69 clearance does not provide immunity to new infections or eliminate the risk of hepatocellular
70 carcinoma in patients with established cirrhosis. Therefore, an effective preventative vaccine
71 is an important medical and public health need (4).

72 The genetic diversity of HCV of at least seven genotypes that differ up to 30% in
73 nucleotide sequence poses a major challenge to developing a pan-genotypic vaccine. HCV is
74 composed of a nucleocapsid core enveloped by a lipid bilayer in which two surface
75 glycoproteins, E1 and E2, are anchored. During acute infection, a robust neutralizing
76 antibody response correlates with spontaneous resolution of infection (5, 6). Most broadly
77 neutralizing antibodies (bNAbs) recognize conformational epitopes in E2 and some in E1E2
78 (7, 8). Passive immunization with anti-HCV antibodies before HCV challenge can prevent
79 infection against homologous virus challenge in animal models (9, 10), although virus
80 breakthrough can occur and protection against heterologous virus strains remains a problem.
81 Other complicating factors for vaccine development include low immunogenicity of viral
82 envelope proteins and antibody responses directed to regions that display a high mutational
83 rate of change (11). In addition, a number of studies have highlighted the role of N-linked
84 glycosylation in masking or shielding E2 epitopes from recognition by bNAbs (12-16), as
85 also observed for HIV and influenza virus (17). Such glycan shielding may hinder bNAb
86 induction by reducing the exposure of neutralizing epitopes to the humoral immune system,
87 further complicating development of a B cell-based HCV vaccine.

88 There is evidence from a number of studies, mainly involving HIV and influenza, that

89 alteration of glycans on viral envelope glycoproteins can impact immune recognition and
90 immunogenicity. Some studies have used hyperglycosylation, the addition of N-glycans
91 through mutagenesis to create glycan sequons, to mask certain sites associated with
92 non-neutralizing antibodies and antibody escape (18-22). Conversely, targeted removal of
93 glycans through mutagenesis of glycan sequons has been used to improve or alter
94 neutralizing antibody engagement of key epitopes for HIV-1 (23-26), influenza A virus (27),
95 and HCV (13-15). For example, in one study, elimination of glycosylation sites in the
96 vicinity of the CD4-binding site of the HIV-1 envelope glycoprotein (Env) generated an
97 immunogen that more efficiently activated B cells expressing germline precursors of bNAbs
98 (25). However, in another study, targeted deglycosylation of HIV-1 Env failed to generate an
99 antigen capable of eliciting neutralizing antibodies against wild-type viruses in immunized
100 guinea pigs or rhesus macaques (28). In the case of influenza A virus, removal of glycans in
101 the hemagglutinin (HA) protein that shield key epitopes of HA from antibody recognition
102 produced immunogens that elicited bNAbs effective against antigenically distant virus
103 strains (27). In the case of HCV, deletion of specific glycans in HCV E1E2 was found to
104 modulate binding of certain bNAbs (14, 15), although the immunogenicity of these modified
105 E1E2 proteins was not studied.

106 An alternate strategy to modulate presentation of key antibody epitopes is
107 modification of the extent of glycosylation through the use of various expression cell types
108 (29-32), or enzymatic truncation of glycoforms (33). In one study, HIV-1 gp120 was
109 produced in *Spodoptera* insect (Sf9) cells, which impart mainly paucimannose type glycans,
110 and in mammalian (HEK293) cells treated with the α -mannosidase inhibitor kifunensine,

111 which confers only high mannose type glycans (30). These global alterations in
112 glycosylation compared to gp120 produced in untreated HEK293 cells led to increased
113 exposure of the CD4 binding site, which encouragingly translated to increased binding of
114 bNAbs specific for this site. However, the effect on HIV-1 neutralization titers in animals
115 immunized with these modified gp120 glycoproteins was not reported. More recently, a
116 secreted, soluble form of HCV E2 (sE2) produced in *Drosophila* insect (S2) cells was found
117 to be more immunogenic than the corresponding protein produced in HEK293 cells (31).
118 Moreover, S2-derived sE2 elicited higher titers of antibodies capable of neutralizing a
119 diverse panel of HCV genotypes, suggesting that distinct glycosylation patterns should be
120 taken into consideration in development of a recombinant HCV vaccine.

121 To further test the hypothesis that differential glycosylation may influence the
122 antigenicity and immunogenicity of E2, we performed head-to-head molecular, antigenic
123 and immunogenic comparisons of sE2 produced in (i) mammalian (HEK293) cells, which
124 impart high mannose, hybrid and complex glycans; and (ii) insect (Sf9) cells, which confer
125 mainly paucimannosidic glycans. In contrast to Li et al. (31), we found that immunization of
126 mice with mammalian and insect sE2 glycoproteins elicited comparable antibody
127 neutralization titers against heterologous HCV isolates, although Sf9-derived sE2 was a
128 more potent immunogen against the homologous H77c isolate. We discuss possible reasons
129 for the apparent discrepancy between our results and theirs, and conclude that targeted
130 deletion of specific E2 glycans, rather than expression system-dependent modification of all
131 glycans, may be a better strategy for increasing the exposure of virus neutralizing epitopes to
132 the humoral immune system.

133

134 **MATERIALS AND METHODS**

135 **Protein expression, purification, and antibodies.** For mammalian cell expression, a
136 gene encoding HCV E2 from strain 1a H77c (residues 384–661) was cloned into the vector
137 pSecTag2 (Invitrogen) with an N-terminal immunoglobulin κ light chain signal sequence (for
138 secretion) and a C-terminal His₆ tag (for purification). The construct was transfected with
139 293fectin into FreeStyle HEK293-F cells (Invitrogen). Recombinant monomeric E2 was
140 purified from culture supernatants by sequential HisTrap Ni²⁺-NTA and Superdex 200 columns
141 (GE Healthcare). For insect cell expression, the same E2 sequence was fused to the gp67
142 secretion signal sequence of baculovirus vector pAcGP67-B (BD Biosciences) with a
143 C-terminal His₆ tag. To generate recombinant baculovirus, this construct was transfected into
144 Sf9 cells together with BaculoGold Linearized DNA (BD Biosciences). Soluble monomeric E2
145 was purified from culture supernatants of Sf9 cells infected with recombinant baculovirus
146 using sequential HisTrap Ni²⁺-NTA and Superdex 200 columns.

147 Human CD81 large extracellular loop (CD81-LEL; CD81 residues 113–201) coding
148 sequence DNA was synthesized (GenScript) and cloned into the vector pHLsec (Addgene
149 plasmid #99845; a gift from E. Yvonne Jones) which includes a C-terminal His₆ tag. The
150 construct was transfected with PEI MAX 40K (Polysciences) into FreeStyle HEK293-F cells.
151 CD81-LEL was purified from culture supernatant by sequential HiTrap Chelating HP
152 Ni²⁺-NTA and Superdex 75 columns (GE Healthcare). Before biolayer interferometry, purified
153 CD81-LEL was stripped of its C-terminal His₆ tag by digestion with carboxypeptidase
154 A-agarose (Sigma).

155 Monoclonal antibody HCV1 was kindly provided by Dr. Yang Wang (MassBiologics,
156 University of Massachusetts Medical School) (37). Monoclonal antibodies against different
157 antigenic domains, CBH-4B and CBH-4G (domain A), HC-1 and HC-11 (domain B), CBH-7
158 (domain C), HC84.24 and HC84.26 (domain D), and HC33.1 and HC33.4 (domain E) were
159 employed and prepared as described (7).

160 **Mass spectrometry.** Digestion was performed on 80 µg each of HEK293- and
161 Sf9-derived sE2 by denaturing using 6 M guanidine HCl, 1 mM EDTA in 0.1 M Tris, pH 7.8,
162 reduced with a final concentration of 20 mM DTT (65 °C for 90 min), and alkylated at a final
163 concentration of 50 mM iodoacetamide (room temperature for 30 min). Samples were then
164 buffer exchanged into 1 M urea in 0.1 M Tris, pH 7.8 for digestion. Sequential digestion was
165 performed using trypsin (1/50 enzyme/protein ratio, w/w) for 18 hours at 37°C, followed by
166 chymotrypsin (1/20 enzyme:protein, w/w) with 10 mM CaCl₂ overnight at room temperature.
167 LC-UV-MS analyses were performed using an UltiMate 3000 LC system coupled to an LTQ
168 Orbitrap Elite equipped with a heated electrospray ionization (HESI) source and operated in a
169 top 5 dynamic exclusion mode. A volume of 30 µl (representing 9 µg of digested protein) of
170 sample was loaded via the autosampler onto a C18 peptide column (AdvanceBio Peptide 2.7
171 µm, 2.1 x 150 mm, Agilent part number 653750-902) enclosed in a thermostatted column oven
172 set to 50 °C. Samples were held at 6 °C while queued for injection. The chromatographic
173 gradient was conducted as described in **Table 1**. Glycan and glycopeptide identification was
174 performed using Byonic software and extracted ion chromatograms used for quantification of
175 glycoforms in Byologic software (Protein Metrics).

176 **Glycoprotein modeling.** Glycans were modeled on the E2 protein structure using
177 Rosetta software (34). Prior to glycan modeling, residues from antigenic domain E were
178 modeled into the structure of E2 core (Protein Data Bank accession code 4MWF) (35) and
179 refined using the FloppyTail method in Rosetta (36). The most abundant glycan at each site
180 was encoded as an IUPAC string and modeled on E2 core using the SimpleGlycosylateMover
181 in Rosetta, followed by the glycan_relax protocol to alleviate clashes involving glycans and
182 energetically unfavorable conformations (using command line flags "-tree_based_min_pack
183 -glycan_relax_refine"). Accessible surface area calculations were performed in Rosetta using
184 the TotalSasa filter, specifying the probe radius using the "-sasa_calculator_probe_radius"
185 command line flag. Percent E2 surface masking by glycans was calculated by dividing the
186 surface accessibility of protein residues in the glycosylated E2 model by the surface
187 accessibility of protein residues in the same model with all glycans removed. Structural
188 visualization was performed in Pymol (www.pymol.org).

189 **Biolayer interferometry.** The interaction of sE2 derived from HEK293 or Sf9 cells
190 with CD81 and human monoclonal antibodies (HMAbs) in IgG format specific for antigenic
191 domains A (CBH-4B, CBH-4G), B (HC-1, HC-11), D (HC84.26, HC84.24), and E (HCV1,
192 HC33.1) (7, 37) was measured using an Octet RED96 instrument and Ni²⁺-NTA biosensors
193 (Pall ForteBio). The biosensors were loaded with 5 µg/mL of purified His₆-tagged sE2 for
194 600 sec, then stabilized with the chemical crosslinker mixture of 0.1 M
195 1-ethyl-3-(3-dimethylaminopropyl)-carbodiimide and 0.025 M N-hydroxysuccinimide (GE
196 Life Sciences) for 60 seconds followed by reaction quenching with 1 M ethanolamine, pH
197 8.0 for 60 sec. Association for 300 sec followed by dissociation for 300 sec against a 2-fold

198 concentration dilution series of each antibody was performed. Data analysis was performed
199 using Octet Data Analysis 10.0 software and utilized reference subtraction at 0 nM antibody
200 concentration, alignment to the baseline, interstep correction to the dissociation step, and
201 Savitzky-Golay fitting. Curves were globally fitted based on association and dissociation to
202 obtain K_D values.

203 **Animal immunization.** CD-1 mice were purchased from Charles River. Prior to
204 immunization, sE2 antigens were formulated with SAS adjuvant (Sigma Adjuvant System,
205 Sigma Aldrich) at a 1:1 ratio according to the manufacturer's instructions. On scheduled
206 vaccination days, groups of 6 female mice, age 7–9 weeks, were injected via the
207 intraperitoneal (IP) route with a 50 μg sE2 prime (day 0) and boosted with 10 μg sE2 on days
208 7, 14, 28, and 35. Blood samples were collected prior to each injection with a terminal bleed
209 on day 49. The collected samples were processed for serum by centrifugation and stored at
210 -80°C until analysis was performed.

211 **Competitive binding ELISA.** An ELISA measured the inhibition by mouse sera of
212 HMAb binding to E2 glycoproteins captured by *Galanthus nivalis* lectin (GNA) (38).
213 Briefly, microtiter plates were coated with GNA and blocked with 2.5% bovine serum
214 albumin (BSA) and 2.5% normal goat serum in 0.1% Tween-PBS, prior to the addition of 2
215 $\mu\text{g}/\text{well}$ of HEK293 sE2. Pretitrated mouse serum was added to each well at a saturating
216 concentration. After 1 h, HMAb was added at a concentration corresponding to 65% to 75%
217 of the maximal optical density (OD) level, incubated for 30 min at either room temperature
218 or 40°C , and then washed. Bound HMAb was detected by incubation with alkaline
219 phosphatase-conjugated goat anti-human IgG (Promega), followed by incubation with

220 p-nitrophenyl phosphate (Sigma) for color development. Absorbance was measured at
221 405/570 nm. This assay was carried out in triplicate, a minimum of two times for each
222 HMAb.

223 **Cell lines and pseudoparticle plasmid construction.** The human embryonic
224 kidney 293T (HEK293T) and Hep3B cells were purchased from ATCC (www.atcc.org).
225 Both HEK293T and Hep3B cells were grown in Dulbecco's modified essential medium
226 (DMEM) (Thermo Fisher Scientific) supplemented with 10% fetal bovine serum (FBS) and
227 1% penicillin-streptomycin (Thermo Fisher Scientific). The human hepatoma cell line,
228 HuH7 was purchased from ECACC and routinely tested for mycoplasma contamination.
229 HuH7 cells were grown in Dulbecco's modified essential medium (DMEM) (Thermo Fisher
230 Scientific) supplemented with 10% fetal bovine serum (FBS) and 1% non-essential amino
231 acids (NEAA) (Thermo Fisher Scientific). All were maintained in a humidified 37 °C, 5%
232 CO₂ incubator. The different genotype constructs for gt1a (H77c, UNKP1.1.1), gt1b
233 (UNKP1.20.3, UNKP1.21.2), gt2a (J6, JFH), gt2b (UNKP2.4.1), gt2i (UNKP2.1.2), gt3
234 (UNKP3.2.2), gt4 (UNKP4.2.1), gt5 (UNKP5.1.1), and gt6 (UNKP6.1.1) were described
235 previously (39, 40). The MLV Gag-Pol packaging vector (phCMV-5349) and luciferase
236 reporter plasmid (pTG126) have been reported (40). All plasmids were grown and purified
237 using the EndoFree Plasmid Maxi Kit (Omega Bio-tek). Concentration and purity were
238 verified by restriction analysis, sequencing and spectrophotometry.

239 **Pseudoparticle generation and titration.** HCV pseudoparticles (HCVpp) were
240 generated by co-transfection of HEK293T cells with the MLV Gag-Pol packaging vector,
241 luciferase reporter plasmid, and plasmid expressing HCVE1E2 using Lipofectamine 3000

242 (Thermo Fisher Scientific) as described previously (40). No-envelope control (empty
243 plasmid) was used as negative control in all experiments. Supernatants containing
244 HCVE1E2 pseudoparticles were harvested at 48 h and 72 h post-transfection, and filtered
245 through 0.45 μm pore-sized membranes. The generated HCVpp is capable of achieving a
246 single-round infection in Hep3B or HuH7 target cells and contains a luciferase reporter gene
247 that can be expressed in infected cells. Titration of HCVpp was then determined by infecting
248 Hep3B cells with a serial dilution.

249 **HCVpp neutralization assays.** For infectivity and neutralization testing of HCVpp,
250 either 10^4 Hep3B cells per well or 1.5×10^4 HuH7 cells per well were plated in white 96-well
251 tissue culture plates (Corning) and incubated overnight at 37 °C. The following day, HCVpp
252 were mixed with appropriate amounts of antibody and then incubated for 1 h at 37 °C before
253 adding to Hep3B or HuH7 cells. After 72 h at 37 °C, either 100 μl Bright-Glo (Promega) was
254 added to each well and incubated for 2 min or cells were lysed with Cell lysis buffer
255 (Promega E1500) and placed on a rocker for 15 min. Luciferase activity was then measured
256 in relative light units (RLUs) using either a SpectraMax M3 microplate reader (Molecular
257 Devices) with SoftMax Pro6 software (Bright-Glo protocol) or wells were individually
258 injected with 50 μL luciferase substrate and read using a FLUOstar Omega plate reader
259 (BMG Labtech) with MARS software. Infection by HCVpp was measured in the presence of
260 anti-HCV E2 MAbs, tested animal sera, pre-immune animal sera, and non-specific IgG at the
261 same dilution. Each sample was tested in duplicate or triplicate. Neutralizing activities were
262 reported as 50% inhibitory dilution (ID_{50}) values and were calculated by nonlinear regression
263 (Graphpad Prism Version 7), using lower and upper bounds (0% and 100% inhibition) as

264 constraints to assist curve fitting.

265 **Statistical analysis.** Comparison of neutralization titers between groups (ID₅₀
266 values; **Figures 8 and 9**) was performed using Kruskal-Wallis ANOVA with Dunn's multiple
267 comparison test. Data analysis was not blinded. Differences were considered statistically
268 significant at $p < 0.05$. Comparison of serum antibody percent E2 binding competition
269 between groups (Figure 7) was performed using t-test. Statistical analyses were performed
270 using GraphPad Prism 7 software.

271

272 RESULTS

273 **Expression of soluble HCV E2 glycoprotein in HEK293 and Sf9 cells.** In order to
274 investigate the effect of different glycosylation patterns on the antigenicity and
275 immunogenicity of HCV E2, we produced a soluble form of E2 (sE2) lacking the
276 hydrophobic C-terminal transmembrane anchor in mammalian (HEK293) and insect (Sf9)
277 cells, which are known to attach different N-glycan moieties to proteins (42, 43). For
278 expression of sE2 in HEK293 cells, a DNA fragment encoding amino acids 384–661 of strain
279 1a HCV H77c polyprotein was cloned into the pSecTag2 vector under control of the CMV
280 promoter. The same DNA fragment was used for expression of sE2 in Sf9 insect cells using
281 the pAcGP67-B vector in which expression is controlled by the polyhedrin promoter (**Figure**
282 **1A**). Secreted, monomeric sE2 proteins bearing C-terminal His₆ tags were purified from
283 culture supernatants by immobilized Ni²⁺ affinity chromatography, followed by size
284 exclusion chromatography. Superdex 200 elution profiles for HEK293- and Sf9-derived sE2
285 showed that both proteins formed oligomers and high molecular aggregates, in addition to

286 monomers (**Figure 1B and C**). In both cases, we isolated the peak corresponding to
287 monomeric sE2. Only monomeric HEK293- and Sf9-derived sE2 proteins were used for all
288 subsequent analytical and immunological experiments. As shown in **Figure 1D**, the
289 HEK293- and Sf9-derived sE2 proteins migrated in non-reducing SDS-PAGE at apparent
290 molecular weights of ~75 kDa and ~40 kDa, respectively, compared to a calculated
291 molecular weight of ~34 kDa based on primary amino acid sequence. Thus, sE2 is
292 glycosylated differently by mammalian and insect cells, as expected (42, 43). In addition, we
293 examined HEK293- and Sf9-derived sE2 in SDS-PAGE under reducing conditions and
294 carried out Western blot analysis using HMAb HC33.1 (**Figure 1E**). HC33.1 recognizes a
295 linear epitope of HCV E2 (domain E) comprising residues 412–423 (7). The Western blot
296 revealed major bands at ~60 kDa and ~40 kDa for reduced HEK293- and Sf9-derived sE2,
297 respectively, which is similar to what was observed under non-reducing conditions (**Figure**
298 **1D**). There was no indication of significant proteolysis of either HEK293- or Sf9-derived
299 sE2 (**Figure 1E**). Moreover, reactivity with HC33.1 confirmed the identity of both purified
300 proteins as HCV E2. We therefore conclude that Sf9-derived sE2 is intact and not more
301 susceptible to proteolysis than HEK293-derived sE2, despite differences in glycosylation. To
302 pinpoint these differences, we used mass spectrometry (MS) to identify the nature of sugars
303 attached to HEK293- and Sf9-derived sE2.

304 **N-glycosylation analysis of HCV E2 expressed in HEK293 and Sf9 cells.** Three
305 major types of mature N-glycans may be attached to glycoproteins such as HCV E2
306 produced in mammalian cells: (i) high mannose glycans, consisting of up to six mannose
307 (Man) residues attached to a trimannosyl chitobiose core (Man₃GlcNAc₂); (ii) complex type

308 glycans, composed primarily of N-acetylglucosamine (GlcNAc) and galactose (Gal)
309 residues attached to the $\text{Man}_3\text{GlcNAc}_2$ core, with or without sialic acid (NeuAc) residues,
310 where a fucose (Fuc) residue may be added to the first GlcNAc of the core; and (iii) hybrid
311 type glycans, which consist of Man and lactosamine (GlcNAcGal) residues, with or without
312 NeuAc, attached to the $\text{Man}_3\text{GlcNAc}_2$ core (42, 43). Insect expression systems, on the other
313 hand, commonly express paucimannose structures as well as core α 1,3 fucosylation absent in
314 mammalian expression systems.

315 We used MS to characterize the glycan moieties attached to the 11 potential
316 N-glycosylation sites of HCV E2 derived from HEK293 and Sf9 cells. The composition and
317 microheterogeneity of the glycans attached to each N-linked site were determined by
318 LC-UV-MS/MS analyses of enzymatic digests (trypsin and chymotrypsin sequential digest)
319 of reduced and alkylated HEK293- and Sf9-derived sE2. Glycopeptide identifications were
320 made based on MS/MS fragmentation, followed by relative abundance calculation using
321 extracted ion chromatograms of the parent ion. Representative MS spectra of glycopeptide
322 447–455 of HEK293- and Sf9-derived sE2 are shown in **Figure 2**. Doubly charged
323 glycopeptides observed above 1% relative abundance are depicted to demonstrate the
324 general trend of glycans of larger composition observed in HEK293-derived sE2. A complete
325 list of the glycan compositions identified at each glycosylation site of HEK293-derived
326 versus Sf9-derived sE2, as well as the corresponding glycan populations down to 0.1%
327 relative abundance based on extracted ion chromatograms of the parent ions, is presented in
328 **Supplementary Table 1**. These 11 glycosylation sites are located at E2 positions 417
329 (designated N1), 423 (N2), 430 (N3), 448 (N4), 476 (N5), 532 (N6), 540 (N7), 556 (N8), 576

330 (N9), 623 (N10), and 645 (N11).

331 Multiple complex and high mannose type glycans were identified at 11 of 11
332 N-linked sites of HEK293-derived sE2 (**Supplementary Table 1**). As expected for a
333 glycoprotein expressed in insect cells (42, 43), the major glycoforms present on Sf9-derived
334 sE2 were paucimannose N-glycans, with or without one or two core Fuc residues. Complex
335 N-glycans were detected at all sites except N7 in Sf9-derived sE2, albeit with a lower degree
336 of extension and branching on average than in HEK293-derived sE2. Complex type glycans
337 accounted for only 1–10% of the total identified N-glycans in Sf9-derived sE2
338 (**Supplementary Table 1**). The most abundant glycoform at each site observed in LC-MS
339 analysis of HEK293- and Sf9-derived sE2 is depicted in **Figure 3**.

340 For both HEK293- and Sf9-derived sE2, the same nine N-glycan sites are near fully
341 (>95%: N1, N2, N4, N5, N6, N8 and N9) or highly (>75%: N3 and N7) glycosylated (**Figure**
342 **4**). Of note, the two exceptions (N10 and N11) exhibit relatively low levels of glycan
343 occupancy in both mammalian and insect cell-derived sE2. This concordance in extent of
344 glycosylation for sE2 from two hosts with significantly different protein N-glycosylation
345 pathways suggests that factors intrinsic to E2 itself, such as differential accessibility of
346 individual glycosylation sites to the cellular N-glycosylation biosynthetic machinery, may
347 explain the observed site-specific differences in percent glycosylation (**Figure 4**).

348 **Molecular modeling of N-glycosylation sites.** To compare the structural impact of
349 N-glycosylation in sE2 derived from HEK293 versus Sf9 cells, we modeled the most
350 abundant glycoform at each site on the E2 core structure (**Figure 5**). This analysis
351 highlighted the differential glycan sizes observed in the two expression systems, particularly

352 those proximal to key epitopes such as N6 (**Figure 5A and B**), which is adjacent to the
353 ARC3 binding site in antigenic domain B (7) and is markedly larger for HEK293- versus
354 Sf9-expressed sE2. These models were used to calculate protein surface occlusion from
355 glycosylation (**Table 2**). Though a solvent-sized probe (1.4 Å radius) detected little
356 difference between E2 surface occlusion in the models, larger probe radii (5 and 10 Å),
357 which are more representative of antibody complementarity-determining region (CDR)
358 loops, revealed relatively high E2 occlusion (40–65% of the protein surface), with
359 HEK293-derived sE2 having somewhat higher levels of masked surface than Sf9-derived
360 sE2 (9% higher for 10 Å probe). This is similar to previous observations comparing
361 glycosylation of HEK293- versus Sf9-expressed HIV gp120, where approximately 10%
362 greater surface occlusion for HEK293-expressed gp120 was calculated using a 10 Å probe
363 radius (30). However, it should be noted that this analysis does not include E2 regions
364 missing from the crystal structure (e.g. HVR1), E2 dimerization with E1, and conformational
365 mobility of glycans and E2 residues. Nevertheless, the calculated 9% reduction in protein
366 surface coverage imparted by the Sf9 cell production system could potentially affect the
367 exposure of antibody binding sites proximal to glycans.

368 **CD81 binding and antigenicity of HCV E2 expressed in mammalian versus**
369 **insect cells.** To determine whether differential glycosylation affected binding to the CD81
370 entry receptor, we used biolayer interferometry (BLI) to measure the affinity of HEK293-
371 and Sf9-derived sE2 for recombinant CD81 (**Figures 6A and B**). Purified sE2 proteins were
372 directionally coupled to a Ni²⁺-NTA biosensor surface through their C-terminal His₆ tags.
373 HEK293-derived sE2 bound CD81 with a K_D of 510 nM compared to 440 nM for

374 Sf9-derived sE2 (**Table 3**). These very similar K_D values demonstrate that both glycoproteins
375 are functional with respect to entry receptor binding. Moreover, this result indicates that the
376 proteins are properly folded since alanine-scanning mutagenesis has shown that the CD81
377 binding site comprises residues from several non-contiguous segments of the E2 polypeptide
378 chain (i.e. it is conformational in nature) (7, 8).

379 To determine whether differential glycosylation affected epitope presentation, we
380 used BLI to measure the binding of HEK293- and Sf9-expressed sE2 to a panel of eight
381 HMAs targeting four antigenic domains on E2: CBH-4B and CBH-4G (domain A), HC-1
382 and HC-11 (domain B), HC84.26 and HC84.24 (domain D), and HCV1 and HC33.1 (domain
383 E) (7, 37) (**Figure 6C–L**). Of note, this provides a direct comparative view of 293- versus
384 Sf9-expressed sE2, while absolute measured affinity (K_D) values may reflect effects of
385 bivalent IgG binding. Five of these HMAs bound both sE2 proteins with very similar K_D s,
386 all in the nanomolar range: HC84.26 (1.8 nM for HEK293-derived sE2; 2.7 nM for
387 Sf9-derived sE2), HCV1 (36 and 9.3 nM), HC33.1 (50 and 47 nM), HC-1 (65 and 69 nM),
388 and HC-11 (7.0 and 25 nM) (**Table 3**). Importantly, the ability of conformation-dependent
389 HMAs HC84.26, HC-1, and HC-11 (7) to recognize both versions of sE2 with high affinity
390 indicates that both glycoproteins are correctly folded, in agreement with our CD81 binding
391 results. The other three HMAs bound HEK293-derived sE2 more tightly than Sf9-derived
392 sE2: HC84.24 (1.9 nM for HEK293-derived sE2; 1200 nM for Sf9-derived sE2), CBH-4B
393 (11 and 120 nM), and CBH-4G (120 nM for HEK293-derived sE2; no apparent binding to
394 Sf9-derived sE2) (**Table 3**). We attribute these affinity differences to differential
395 glycosylation, given that glycans cover ~50% of the surface of sE2 (**Figure 2**) and so are

396 likely to influence HMAb binding to at least some epitopes, either directly or indirectly (see
397 Discussion). These results demonstrate that increasing protein surface exposure by reducing
398 glycan size did not translate into enhanced antigenicity, at least for the eight HMABs tested
399 here.

400 **Immunization of mice with sE2 induces serum antibodies that recognize**
401 **broadly neutralizing epitopes.** To compare the antibody responses in mice immunized
402 with the HEK293- and Sf9-derived sE2 proteins, groups of CD-1 mice (n=5) were
403 immunized with 50 µg of purified protein formulated in SAS adjuvant (oil-in-water
404 emulsion), followed by four 10 µg boosts over a course of five weeks. Serum samples were
405 collected one week after the fifth immunization (D=42), and sera tested for epitope-specific
406 responses by competitive binding ELISA using HMABs derived from HCV-infected
407 individuals that represent the five antigenic domains of E2 (7-10): CBH-4B (domain A),
408 HC-1 (domain B), CBH-7 (domain C), HC84.26 (domain D), and HC33.3 (domain E)
409 (**Figure 7**). Based on binding competition, antibodies were elicited to all five antigenic
410 domains in both groups of mice. Both groups had relatively high levels of serum competition
411 with the antigenic domain B HMAb HC-1; this domain is associated with broadly
412 neutralizing antibodies and overlaps with the CD81 binding site (7). Comparing the two
413 groups of immunized mice, no significant differences were observed for domain-specific
414 serum antibody competition (t-test, GraphPad Prism 7).

415 **Viral neutralization against homologous and heterologous isolates of HCV.** In
416 order to assess the relative potency of the HEK293- and Sf9-derived sE2 immunogens,
417 mouse sera were tested for neutralizing antibody (nAb) titers against homologous and

418 heterologous isolates of HCV E1E2 using the HCVpp neutralization assay. The values are
419 expressed as serum dilution levels corresponding to 50% neutralization (ID_{50}). As shown in
420 **Figure 8**, the mean ID_{50} values of nAb against the homologous isolate (H77c) (i.e. same
421 E1E2 sequences as used in the vaccine) were 5-10 fold higher for Sf9-derived versus
422 HEK293-derived sE2 after the third (D=28), fourth (D=35), and fifth (D=42) immunizations,
423 with significant differences between groups at Days 28 and 42. However, the difference
424 diminished two weeks after the last immunization (D=49) to give approximately the same
425 values.

426 To assess the breadth of neutralization, mouse sera (Day 49) were subsequently
427 tested against a diverse panel of six HCV genotypes: gt1a, gt1b, gt2a, gt2b, gt2i, gt3a, gt4a,
428 gt5a, and gt6a, as previously described (40). As shown in **Figure 9**, animals immunized with
429 both HEK293- and Sf9-derived sE2 were able to elicit bNAbs against all of the HCVpps
430 tested in the panel, although genotypes 1a and 1b had the highest ID_{50} titers overall. The ID_{50}
431 values against the homologous H77c isolate were moderately, though not significantly,
432 higher for Sf9-derived sE2. This confirms the relative H77c neutralization titers observed at
433 this timepoint in **Figure 8**, which was performed separately using different target cells
434 (Hep3B cells, versus HuH7 cells for **Figure 9**). For most of the other isolates, there were
435 modest, though insignificant increases of ID_{50} s for the HEK293 sE2 immunized group, with
436 the exception of the J6 isolate where a significant increase for the HEK293 sE2 titers was
437 observed. It is possible that this modest decrease in breadth could be due to a more
438 pronounced nAb response to HVR1 or other variable regions induced by Sf9-expressed sE2
439 versus HEK293-expressed sE2. HVR1 has been reported as an immunodominant site for

440 nAbs, although the nAb response is largely strain-specific (44-47). Therefore, the lower level
441 of ID₅₀ values for the other heterologous HCVpp genotypes may reflect lack of nAb
442 cross-recognition of the HVR1 sites due to sequence variation in this region.

443

444 **DISCUSSION**

445 In this study, we asked whether reducing the overall glycosylation of HCV sE2 (gt1a,
446 H77) by producing this protein in *Spodoptera* insect (Sf9) cells improved its antigenicity
447 and/or immunogenicity compared to sE2 produced in mammalian (HEK293) cells. Mass
448 spectrometry showed that all 11 predicted N-glycosylation sites were utilized in sE2 from
449 both HEK293 and Sf9 cells. Although most sites were fully or nearly fully glycosylated, two
450 sites (N10 and N11) showed low (<50%) glycan occupancy. As expected, N-glycans in
451 insect sE2 were, on average, smaller and less complex than N-glycans in mammalian sE2.

452 After modeling the most abundant glycoform at each site on the E2 structure (35), we
453 quantified glycan coverage by calculating the amount of protein surface exposed to a
454 spherical probe the size of an antibody binding site. Our analysis revealed that 64% of the
455 surface of HEK293-derived sE2 was occluded by N-glycans compared to 55% for
456 Sf9-derived sE2, corresponding to a 9% reduction in glycan shielding in insect
457 cell-expressed material. However, this reduction was not associated with improved HMAb
458 binding (**Table 3**). The ability of CD81, HC84.26, HCV1, HC33.1, HC-1 and HC-11 to bind
459 HEK293- and Sf9-derived sE2 equally well indicates that E2 recognition by these six ligands
460 does not require complex type glycans.

461 By contrast, HC84.24, CBH-4B and CBH-4G bound Sf9-derived sE2 less well than
462 HEK293-derived sE2. It is not particularly surprising that some HMABs bind these two
463 glycoproteins with different K_{DS} given that: 1) Sf9- and HEK293-derived sE2 are
464 glycosylated quite differently; 2) glycans cover ~50% of the surface of E2 (**Figure 5**) and so
465 are likely to influence HMAb binding to at least some epitopes, either directly by forming
466 part of such epitopes or indirectly by being proximal to them; 3) the glycosylation profile of
467 natural E2 (i.e. E2 produced in HCV-infected human liver cells) is probably more similar to
468 that of HEK293-derived sE2 than of Sf9-derived sE2; and 4) the HMABs used in this study
469 were derived from individuals naturally infected with HCV. A previous global epitope
470 mapping study (7) found that mutation of certain E2 glycan sites, including glycan N10
471 which is located in the E2 back layer near the mapped CBH-4B and CBH-4G binding sites
472 (**Figure 5**) and shows reduced occupancy for Sf9-expressed sE2 (**Figure 4**), affects E2
473 binding for these and other HMABs. More revealing with respect to structural and functional
474 integrity is the ability of Sf9- and HEK293-derived sE2 to bind the CD81 receptor with
475 nearly identical K_{DS} (**Figure 6A and B**).

476 As observed for recombinant HIV-1 envelope trimer produced in HEK293 cells (23),
477 our LC-UV-MS/MS analysis of HEK293-derived sE2 revealed the presence of
478 under-processed N-glycans that remain in oligomannose form ($\text{Man}_{5-9}\text{GlcNAc}_2$), possibly
479 because the high density of glycans on the E2 surface imposes steric constraints that limit the
480 actions glycan-processing enzymes in the Golgi compartment. We detected high mannose
481 N-glycans at all 11 N-linked sites of HEK293-derived sE2. However, except at sites N8 and
482 N11, the large majority of total identified glycoforms at the other nine N-linked sites were

483 complex type glycans, which are a hallmark of passage through the Golgi apparatus. In this
484 respect, the overall glycosylation profile of HEK293-expressed sE2 resembles that of E1E2
485 heterodimers associated with HCV pseudoparticles (HCVpp), which also display a majority
486 of complex type glycans (16, 48). By contrast, E1E2 heterodimers associated with cell
487 culture-derived HCV (HCVcc) contain a more balanced mixture of high mannose and
488 complex type glycans. This difference suggests that both HEK293-expressed sE2 and
489 HCVpp-associated E1E2 are more accessible to Golgi glycan-processing enzymes than
490 HCVcc-associated E1E2, possibly because, in the HCVcc system, the E1E2 glycoprotein is
491 associated with nascent viral particles as it travels through the secretory pathway, thereby
492 restricting its exposure to Golgi enzymes.

493 In a previous study of HCV sE2 produced in mammalian (CHO) cells (49), complex
494 glycans were detected at only 2 of 11 N-linked sites (N2 and N3); all 9 other sites were
495 occupied by high or paucimannose N-glycans. By contrast, we identified complex glycans at
496 all 11 N-linked sites. Moreover, a complex glycan was the most abundant glycoform at 6 of
497 these 10 sites (N1, N3, N4, N5, N6, and N9) (**Figure 3**). These surprisingly large differences
498 in glycosylation profiles may result from the use of different mammalian cell lines for sE2
499 expression: HEK293 here versus CHO in the earlier study (49). The substantially higher
500 content of complex N-glycans in HEK293-derived sE2 indicates more extensive processing
501 of oligomannoses during passage of this particular glycoprotein through the Golgi
502 compartment of HEK293 than CHO cells.

503 We found that differences in N-glycosylation of sE2 produced in HEK293 versus Sf9
504 cells did not appreciably alter recognition by most HMABs. Immunogenicity studies in mice

505 showed that similar polyclonal antibody responses were elicited against domains A–E by
506 competition binding analysis. Neutralizing antibody titers showed that Sf9-derived sE2 was
507 a more potent immunogen than HEK293-derived sE2 when tested against the homologous
508 H77c isolate. However, both HEK293- and Sf9-derived sE2 elicited robust neutralizing
509 antibody titers when tested against a diverse panel of HCVpp genotypes, although the overall
510 titers trended higher for HEK293-derived sE2.

511 Our results differ markedly from those reported previously in a comparison of
512 HEK293- and *Drosophila* S2-derived sE2 (31). In that study, the insect material was found to
513 be a more potent immunogen against a diverse panel of heterologous isolates. Whether or not
514 there is a difference in glycosylation between E2 proteins derived from *Drosophila* versus
515 *Spodoptera* cells that could affect immunogenicity is an open question. At present, most
516 knowledge of insect glycobiology comes from the *Drosophila* model (43), and it cannot be
517 excluded that glycosylation in *Spodoptera* may differ in certain aspects. However, our
518 LC-UV-MS/MS analysis of Sf9-expressed sE2 revealed a glycosylation pattern dominated
519 by paucimannose N-glycans, with or without one or two core fucose residues, which is
520 entirely consistent with what would be expected for sE2 produced in S2 cells (42, 43).
521 Therefore, it is unlikely that differences in N-glycosylation can explain the apparent ability
522 of S2-derived sE2, but not Sf9-derived sE2, to elicit higher titers of bNAbs against diverse
523 HCV genotypes than HEK293-derived sE2 (31).

524 Several other factors may be responsible for the discrepancy between our results and
525 those of Li et al. (31). One is the different mouse strains used here (CD-1) and in the Li et al.
526 study (BALB/c). Although CD-1 mice are outbred and have more genetic diversity than

527 inbred BALB/c mice, this likely did not contribute to the differences seen between the two
528 studies because in this study the B cell responses to sE2 are similar using CD-1 and BALB/c
529 mice (data not shown). It is also possible that the different adjuvants used by us (SAS) and Li
530 et al. (31) (alum/CpG) significantly affected the immune response to otherwise very similar
531 insect cell-derived sE2 glycoproteins. For example, in a study comparing enzymatically
532 demannosylated HIV-1 gp120 produced in CHO cells with its untreated counterpart,
533 demannosylation was found to increase immunogenicity in an adjuvant-dependent manner.
534 Thus, when administered in alum, demannosylated gp120 was more immunogenic than the
535 untreated glycoprotein, but this difference disappeared when Quil-A, a saponin-based
536 adjuvant, was used (50). In this study, we used SAS as the adjuvant, which is an oil-in-water
537 emulsion compared to alum/CpG used by Li et al. (31). It has been previously reported that
538 innate and adaptive immune responses can differ between the two adjuvant systems
539 depending on the antigen used, route of administration, and schedule (51). Nevertheless,
540 both adjuvant systems are capable of eliciting robust B cell responses so this also may not
541 account for the breadth of neutralization differences seen between the two studies. Another
542 difference with the Li et al. study and ours is that our sE2 protein was derived from the gt1a
543 isolate, H77, while their sE2 was from the gt1b isolate, Con1b. These have 22% sequence
544 divergence at the amino acid level, which may impact immunogenicity of specific epitopes
545 or E2 overall; recent studies have demonstrated that HVR1 (amino acid divergence is 59% in
546 that region between H77 and Con1b, with 16 out of 27 amino acids changed) and other E2
547 sites are responsible for differences in neutralization sensitivity for sets of E2-targeting
548 bnAbs (52, 53). Finally, we tested neutralization using HCVpp, whereas Li et al. (31) used

549 HCVcc. This difference is potentially significant because, as noted above, HCVpp and
550 HCVcc have different glycosylation profiles (16, 48). Any one or any combination of the
551 above differences could account for the discrepancies between the two studies.

552 While conceptually very appealing, the idea that altering glycans on viral envelope
553 glycoproteins can actually yield superior immunogens for vaccine development remains to
554 be demonstrated, despite considerable effort by a number of laboratories and some promising
555 results. For example, although HIV-1 gp120 produced in Sf9 cells displayed increased
556 binding to antibodies targeting the CD4 binding site (30), the new generation of HIV-1
557 envelope trimers for vaccine use is expressed in mammalian, not insect, cells (54). Similarly,
558 antigens based on HIV-1 envelope glycan deletion mutants have proved to be less effective
559 than, or at best equivalent to, wild-type antigens at generating neutralizing antibody
560 responses possessing both breadth and potency (17, 28, 55, 56). At present, selective
561 deglycosylation of HIV-1 envelope trimers is under investigation as a strategy for activating
562 naïve B cells expressing germline precursors of antibodies that target the CD4 binding site
563 (25, 26). Given our findings that global alteration of HCV E2 glycosylation by expression in
564 different cellular hosts did not appreciably affect antigenicity or overall immunogenicity,
565 future efforts will focus on complete deletion, rather than only modification, of specific
566 N-glycans in order to increase the exposure of virus neutralizing epitopes on E2 to the
567 humoral immune system. For example, the removal of N-glycans at E2 positions 417 (N1)
568 and 532 (N6) has led to increased sensitivity of the mutant isolates to neutralization by MAbs
569 to antigenic domain E and B, respectively (14, 15). A focused effort to eliminate these and

570 other glycans that affect antibody binding to domains B, D and E might lead to an improved
571 immunogen to elicit their associated bNAbs.

572

573

574 **ACKNOWLEDGMENTS**

575 This work was supported by the National Institutes of Health Grants R01AI132213 (to
576 T.R.F., R.A.M., S.K.H.F., and B.G.P.), R21AI126582 (to S.K.H.F., B.G.P., and R.A.M.) and
577 U19AI123862 (to S.K.H.F.), start-up funding from the University of Maryland (to B.G.P.),
578 MPower funds from the State of Maryland, EU FP7 Grant ‘HepaMAb’ 305600 (to J.K.B.),
579 and MRC Grant G0801169 (to J.K.B.). J.D.G. was supported in part by the University of
580 Maryland Virology Program graduate training grant (NIH T32AI125186). We thank Yang
581 Wang (MassBiologics, University of Massachusetts Medical School) for providing HCV1
582 monoclonal antibody. Certain commercial equipment, instruments, or materials are
583 identified to adequately specify the experimental procedure. Such identification does not
584 imply recommendation or endorsement by the National Institute of Standards and
585 Technology, nor does it imply that the materials or equipment identified are necessarily the
586 best available for the purpose.

587

588 **FIGURE LEGENDS**

589 **Figure 1.** Expression of soluble HCV E2 (sE2) derived from mammalian (HEK293) and
590 insect (Sf9) cells. (A) Schematic representation of sE2 expression cassettes used in
591 mammalian (HEK293-sE2) and insect cell (Sf9-sE2) vectors. A sequence encoding sE2
592 (amino acids 384–661) from genotype 1a (H77) was cloned into the vector pSecTag2
593 in-frame with an immunoglobulin light chain κ signal peptide sequence and fused with a
594 C-terminal His₆ tag. Recombinant plasmid was used to transfect HEK293F cells. The same
595 sequence was cloned into the baculovirus expression vector pAcGP67-B with a polyhedrin
596 (Polh) promoter. The construct was transfected into Sf9 cells together with BaculoGold
597 Linearized to produce sE2. (B) Superdex 200 size exclusion chromatography profile of
598 HEK293-derived sE2 following HisTrap Ni²⁺-NTA affinity chromatography. Peak (red
599 arrow) corresponding to monomeric sE2 was isolated for analytical and immunization
600 studies. (C) Superdex 200 chromatography profile of Sf9-derived sE2 following HisTrap
601 Ni²⁺-NTA chromatography. Peak (red arrow) corresponding to monomeric sE2 was isolated
602 for all further experiments. Peak marked by red arrow corresponds to monomeric sE2. (D)
603 Non-reducing SDS-PAGE (10%) of purified HEK293- and Sf9-derived sE2 proteins used for
604 analytical characterization and immunization studies (Coomassie blue G-250 staining). (E)
605 Western blot analysis of purified HEK293- and Sf9-derived sE2 proteins. Proteins were
606 separated on SDS-PAGE (4–15%) after reduction by β -mercaptoethanol and boiling for 10
607 min. Proteins were then transferred onto a nitrocellulose membrane (Bio-Rad Laboratories).
608 The membrane was probed with anti-HCV E2 HMAb HC33.1 (7) at 4.5 μ g/ml, followed by
609 secondary goat anti-human IgG-HRP conjugate at 1:5000 dilution.

610

611 **Figure 2.** Representative ESI-MS of chymotryptic peptide FNSSGCPER (amino acids 447–
612 455) from HCV sE2. (A) Glycopeptide heterogeneity observed on FNSSGCPER peptide
613 from HEK293-expressed sE2 (RA \geq 1% listed in spectrum and RA \geq 0.1% listed in table).
614 (B) Glycopeptide heterogeneity observed on FNSSGCPER peptide in Sf9-expressed E2 (RA
615 \geq 1% listed in spectrum and RA \geq 0.1% listed in table). Note that only doubly charged
616 glycopeptides are labeled in the spectrum for clarity for both panels (A) and (B).

617

618 **Figure 3.** Schematic representation of HCV sE2 chymotryptic glycopeptides depicted with
619 the most abundant glycan observed during LC-MS analysis of HEK293 (top glycoform) and
620 Sf9 (bottom glycoform) sE2 proteins. In cases where the most abundant proteoform was
621 aglycosylated, the most abundant glycosylated form was used (**Supplementary Table 1**).
622 “...” represents flanking amino acid sequence not shown for brevity. N-acetylglucosamine,
623 blue squares; fucose, red triangles; mannose, green circles; galactose, yellow circles; sialic
624 acid, purple diamonds.

625

626 **Figure 4.** Comparison of percent glycosylation of N-glycan sites for mammalian
627 cell-expressed (HEK293) and insect cell-expressed (Sf9) sE2 glycoproteins. Most N-glycan
628 sites are fully or nearly fully glycosylated, with the exception of N10 (N623) and N11
629 (N645), where N-glycan sites have relatively lower glycan occupancy for Sf9-derived sE2,
630 whereas glycan N3 (N430) has lower glycan occupancy in HEK293 cells.

631

632 **Figure 5.** Modeled structural impact of glycosylation for HEK293- versus Sf9-expressed
633 sE2. Structures of the most abundant glycoforms for HEK293 (A, C) and Sf9 (B, D) sE2
634 were modeled using Rosetta (36) onto the E2 core crystal structure (PDB code 4MWF) (35).
635 Glycans are shown as tan, slate, and yellow sticks and labeled, and E2 is shown as surface
636 and cartoon, with views of E2 front layer (A, B) and back layer (C, D). For reference,
637 neutralizing antibody footprints on E2 are colored blue, magenta, and green, based on the
638 epitope-bound crystallographic structures of HC33.1 (PDB code 4XVJ), AR3C (PDB code
639 4MWF), and HC84.26.5D (PDB code 4Z0X) antibodies, respectively. Colored E2 residues
640 indicate those within 5.0 Å of bound antibody, and shared E2 contact residues between
641 antibodies are colored according to antibody with highest E2 residue burial. Residues from
642 antigenic domain E were modeled at the N-terminus of the E2 core structure using Rosetta
643 (36). Glycan N5, which is within a region that is missing from the E2 core crystal structure, is
644 not shown.

645

646 **Figure 6.** BLI analysis of CD81 and antibody binding to HCV sE2 from HEK293 and Sf9
647 expression systems. (A) Sensograms (left) for CD81 binding to immobilized
648 HEK293-derived sE2. CD81 concentrations were 5000, 4000, 2500, 2000, 1250, 1000, 625,
649 500, 312.5, 250, 156.25, 125, 78.125, 62.5, 39.06 nM. Steady state analysis graph (right)
650 gave $K_D = 510 \pm 22$ nM. (B) Sensograms (right) for CD81 binding to immobilized
651 Sf9-derived sE2. CD81 concentrations were 5000, 4000, 2500, 2000, 1250, 1000, 625, 500,
652 312.5, 250, 156.25, 125, 78.125, 62.5, 39.06 nM. Steady state analysis graph (right) gave K_D
653 $= 440 \pm 38$ nM. (C) Sensograms (left) for HC84.26 (domain D-specific HMAb) binding to

654 immobilized HEK293-derived sE2. HC84.26 concentrations were 5, 2.5, 1.25, 0.625, 0.3125
655 and 0.156 nM. Steady state analysis graph (right) gave $K_D = 1.8 \pm 0.5$ nM. (D) Sensograms
656 (left) for HC84.26 binding to immobilized Sf9-derived sE2. HC84.26 concentrations were
657 10, 5, 2.5, 0.625, 0.3125 and 0.156 nM. Steady state analysis graph (right) gave $K_D = 2.7 \pm$
658 0.8 nM. (E) Sensograms (left) for HC84.24 (domain D-specific HMAb) binding to
659 immobilized HEK293-derived sE2. HC84.24 concentrations were 20, 15, 10, 7.5, 5, 3.75,
660 2.5, 1.875, 0.9375, 0.625, 0.469, 0.3125, 0.234 and 0.156 nM. Steady state analysis graph
661 (right) gave $K_D = 1.9 \pm 0.3$ nM. (F) Sensograms (left) for HC84.24 binding to immobilized
662 Sf9-derived sE2. HC84.24 concentrations were 1000, 750, 500, 375, 250, 187.5, 125, 93.8,
663 62.5, 46.9, 31.6 and 23.4 nM. Steady state analysis graph (right) gave $K_D = 1200 \pm 290$ nM.
664 (G) Sensograms (left) for CBH-4B (domain A-specific HMAb) binding to immobilized
665 HEK293-derived sE2. CBH-4B concentrations were 100, 50, 25, 12.5, 6.25 and 3.125 nM.
666 Steady state analysis graph (right) gave $K_D = 11 \pm 1.7$ nM. (H) Sensograms (left) for
667 CBH-4B binding to immobilized Sf9-derived sE2. CBH-4B concentrations were 50, 25,
668 12.5, 6.25 and 3.13 nM. Steady state analysis graph (right) gave $K_D = 120 \pm 11$ nM. (I)
669 Sensograms (left) for HCV1 (domain E-specific HMAb) binding to immobilized
670 HEK293-derived sE2. HCV1 concentrations were 200, 150, 100, 75, 50, 37.5 and 25 nM.
671 Steady state analysis graph (right) gave $K_D = 36 \pm 3.0$ nM. (J) Sensograms (left) for HCV1
672 binding to immobilized Sf9-derived sE2. HCV1 concentrations were 25, 20, 15, 10, 5, 2.5,
673 1.25 and 0.078 nM. Steady state analysis graph (right) gave $K_D = 9.3 \pm 2.0$ nM. (K)
674 Sensograms (left) for HC-1 (domain B-specific HMAb) binding to immobilized
675 HEK293-derived sE2. HC-1 concentrations were 200, 175, 150, 75, 50, 37.5, 25, 12.5, 6.25,

676 3.125, 1.56, 0.78, 0.39 and 0.195 nM. Steady state analysis graph (right) gave $K_D = 65 \pm 10$
677 nM. (L) Sensograms (left) for HC-1 binding to immobilized Sf9-derived sE2. HC-1
678 concentrations were 200, 175, 150, 75, 50, 37.5, 25, 12.5, 6.25, 3.125, 1.56, 0.78, 0.39 and
679 0.195 nM. Steady state analysis graph (right) gave $K_D = 69 \pm 6.5$ nM.

680

681 **Figure 7.** Competition binding analysis of immune sera corresponding to domains A–E. (A)
682 HEK293-derived sE2 immunized CD-1 mice. (B) Sf9-derived sE2 immunized CD-1 mice.
683 Sera from day 42 were tested for binding competition using antibodies representing antigenic
684 domains A–E (7), with mean percent competition shown with black bars. All values were
685 normalized by subtracting percent competition values from control (pre-immune) sera,
686 which were measured individually for each mouse. Antibodies tested were CBH-4B (domain
687 A), HC-1 (domain B), CBH-7 (domain C), HC84.26 (domain D), and HC33.4 (domain E).

688

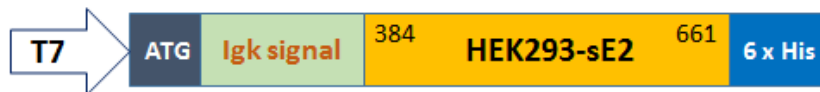
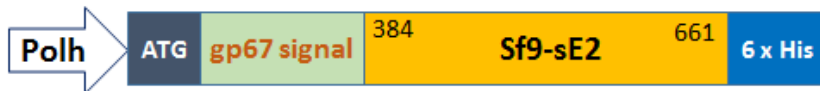
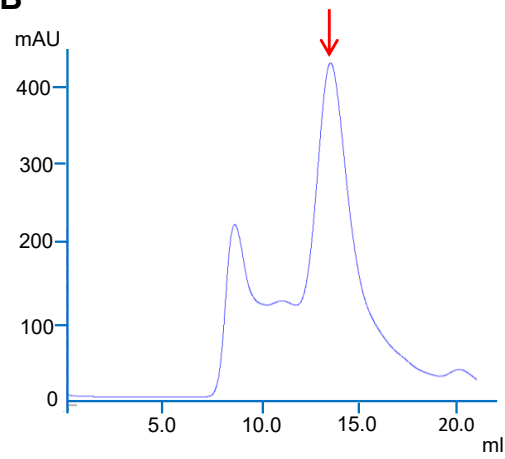
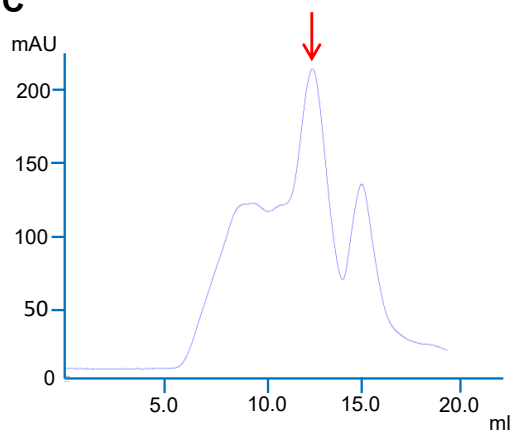
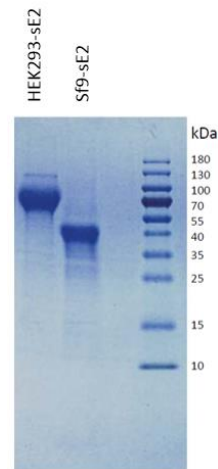
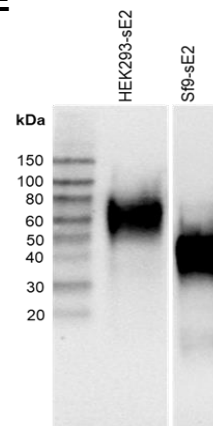
689 **Figure 8.** Kinetics and magnitude of nAb titers against homologous H77 strain. HCV
690 pseudoparticles (HCVpp) were generated by co-transfection of HEK293T cells with HCV
691 E1E2, MLV Gag-Pol packaging vector, and luciferase reporter plasmid as previously
692 described (40). Titrations of HCVpp were performed on Hep3B cells, and luciferase activity
693 measured in relative light units (RLUs) using SpectraMax M3. Percent neutralization was
694 calculated as $100 \times [1 - \text{yRLU}_{\text{test}}/\text{RLU}_{\text{control}}]$. nAb titers in animal sera are reported as
695 50% inhibitory dilution (ID_{50}) values, calculated using nonlinear curve fitting in GraphPad
696 Prism. Neutralization kinetics were determined by inhibition of homologous HCVpp (H77)
697 using serial dilutions of serum collected on days 28, 35, 42 and 49. Blue dots represent serum

698 samples from HEK293 sE2 immunized mice, green dots represent samples from Sf9 sE2
699 immunized mice, and black bars indicate geometric means. One Sf9 E2 immunized mouse
700 had insufficient day 35 sera available for testing, thus four rather than five points are shown
701 for that group and day. P-values were determined using GraphPad Prism 7 with
702 Kruskal-Wallis ANOVA, and significant p-values between immunized groups are indicated
703 (*: $p < 0.05$).

704

705 **Figure 9.** Breadth of neutralization against HCV genotypes 1–6. HCVpp generated with
706 functional E1E2 clones derived from six diverse HCV genotypes, gt1a (H77c, UNKP1.1.1),
707 gt1b (UNKP1.20.3, UNKP1.21.2), gt2a (J6, JFH), gt2b (UNKP2.4.1), gt2i (UNKP2.1.2), gt3
708 (UNKP3.2.2), gt4 (UNKP4.2.1), gt5 (UNKP5.1.1), and gt6 (UNKP6.1.1), were assessed for
709 their neutralization sensitivity (50% neutralization titer; ID₅₀) to CD-1 mouse serum samples
710 immunized with HEK293-derived sE2 (blue dots) and Sf9-derived sE2 (green dots), using
711 HuH7 target cells. Geometric mean ID₅₀ values are shown as black bars. P-values were
712 determined using GraphPad Prism 7 with Kruskal-Wallis ANOVA, and significant p-values
713 between immunized groups are indicated (*: $p < 0.05$).

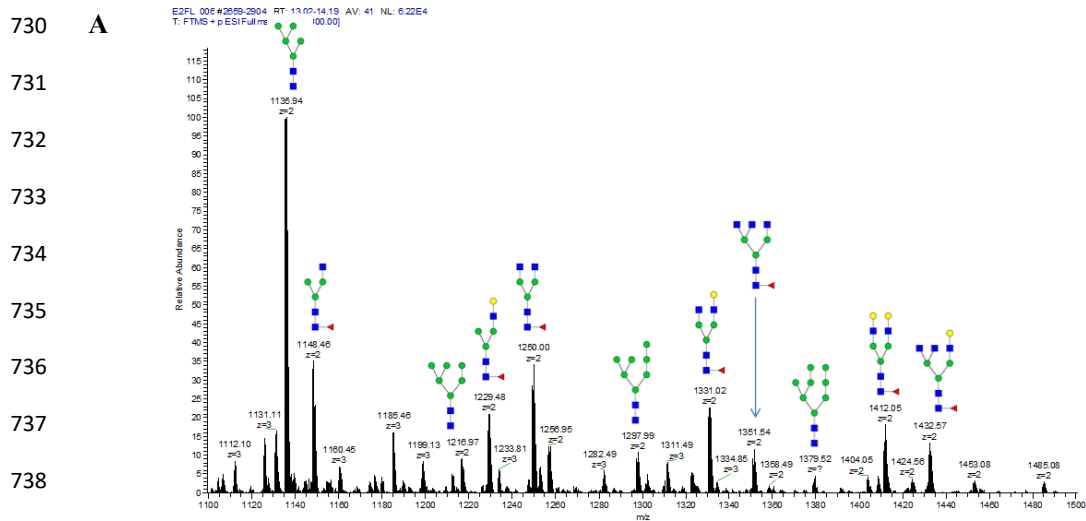
714

715 **Figure 1.**716 **A**717 **pSecTag2 B-HEK293-sE2**719 **pAcGP67 A-Sf9-sE2**721 **B**724 **C**727 **D**730 **E**

733

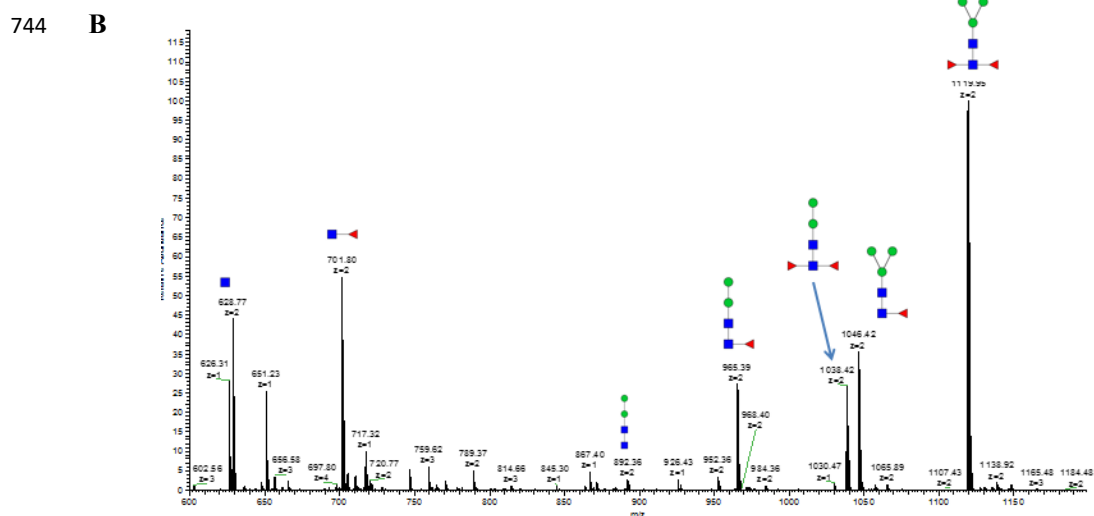
734

729 **Figure 2.**



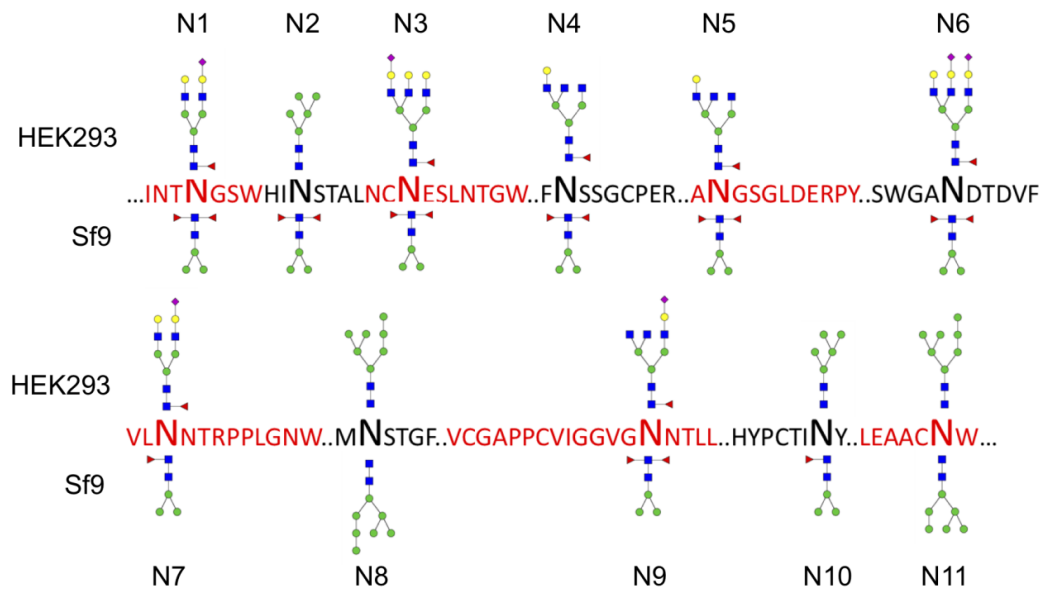
Glycopeptide % relative abundance observed on FNSSGCPER peptide in HEK expressed E2.

															Aglycosylated
17.4	1.47	1.27	0.29	0.49	4.95	10.2	2.27	10.5	10.6	4.43	23.1	8.74	3.86	0.36	



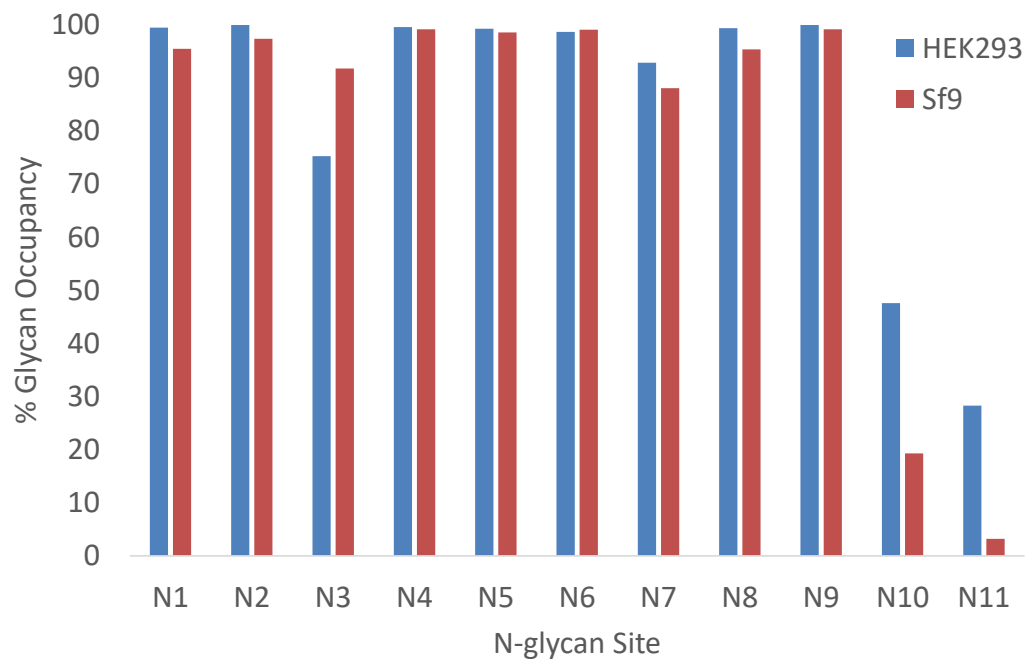
Glycopeptide % relative abundance observed on FNSSGCPER peptide in Sf9 expressed E2.

														Aglycosylated
0.35	0.09	5.7	9.65	1.39	7.22	0.39	0.91	10.66	0.28	12.74	49.85	0.78		

745 **Figure 3.**

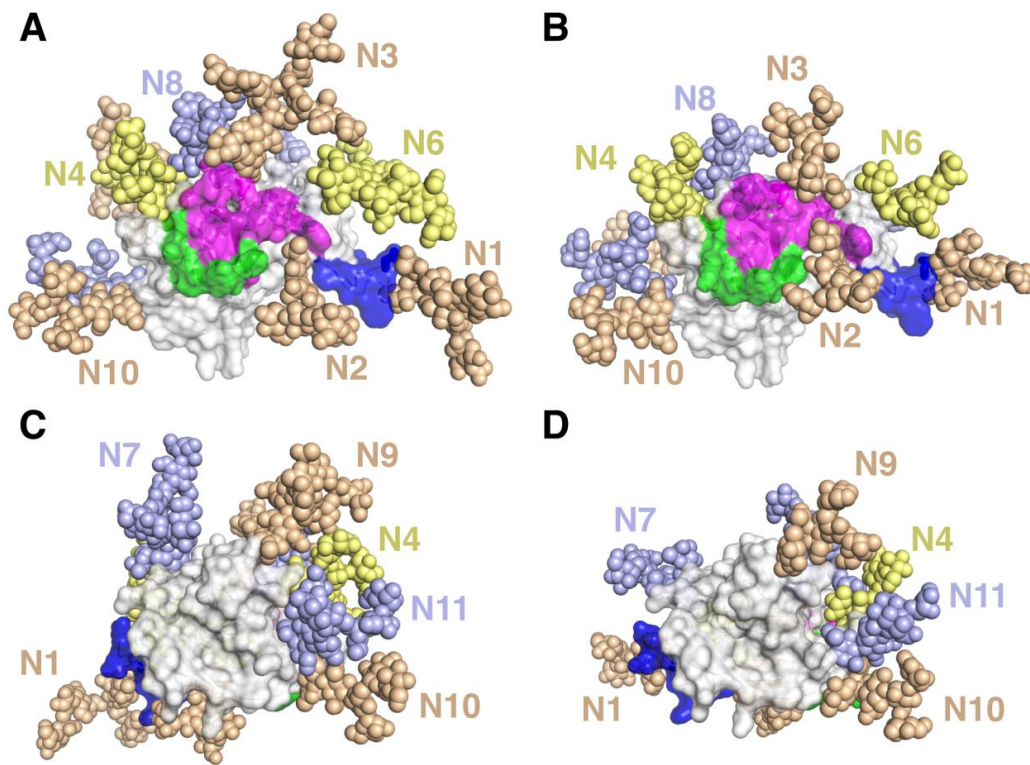
746

747

748 **Figure 4.**

749

750

751 **Figure 5.**

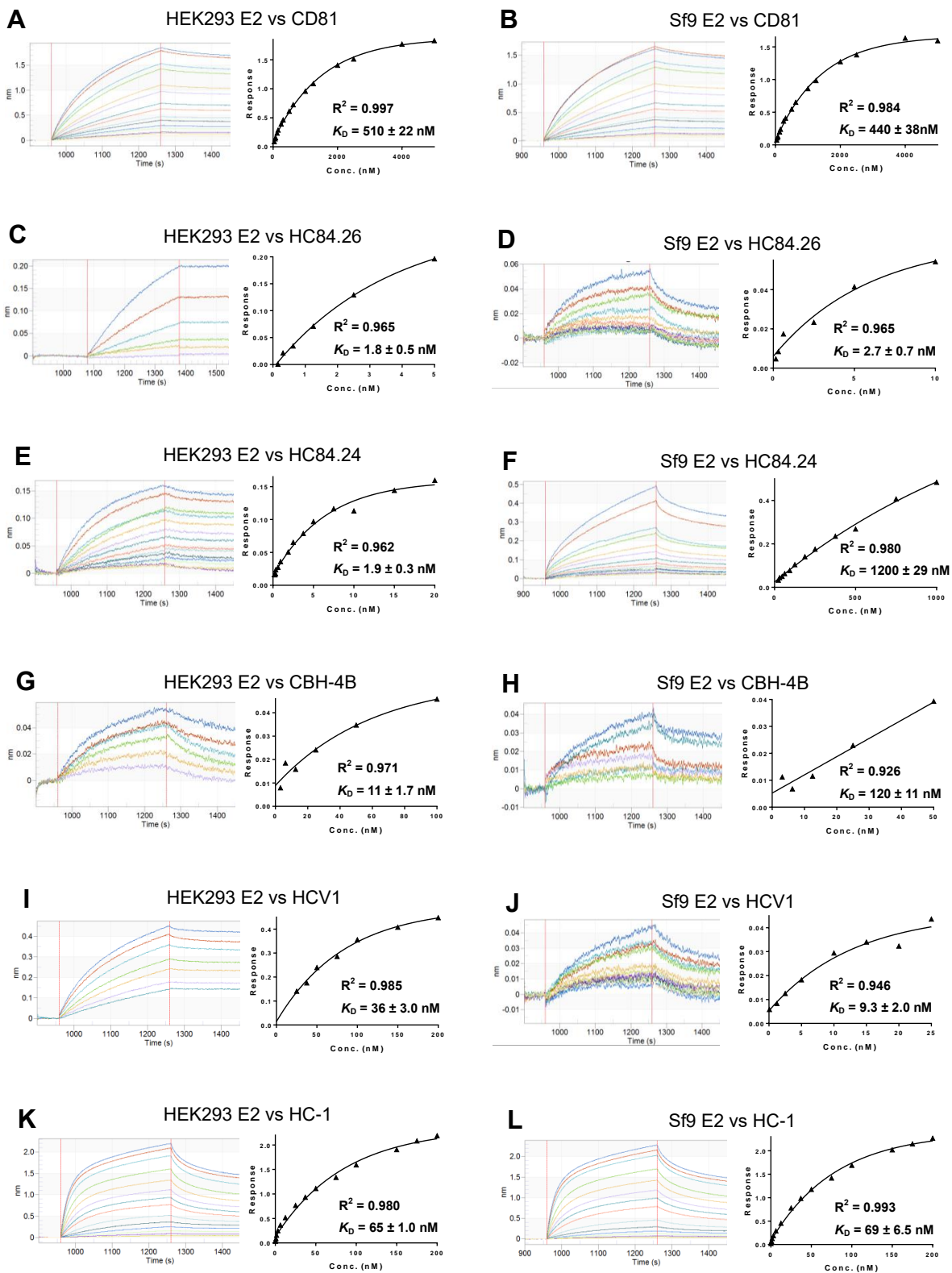
752

753

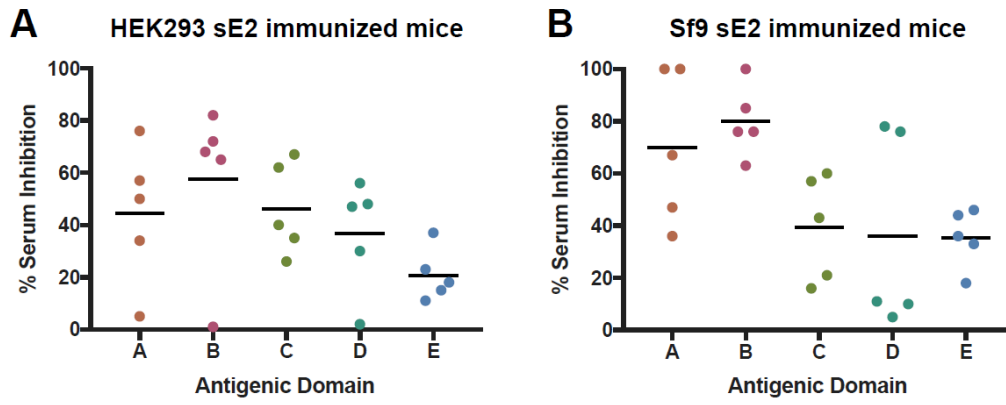
754

755

Figure 6.



40

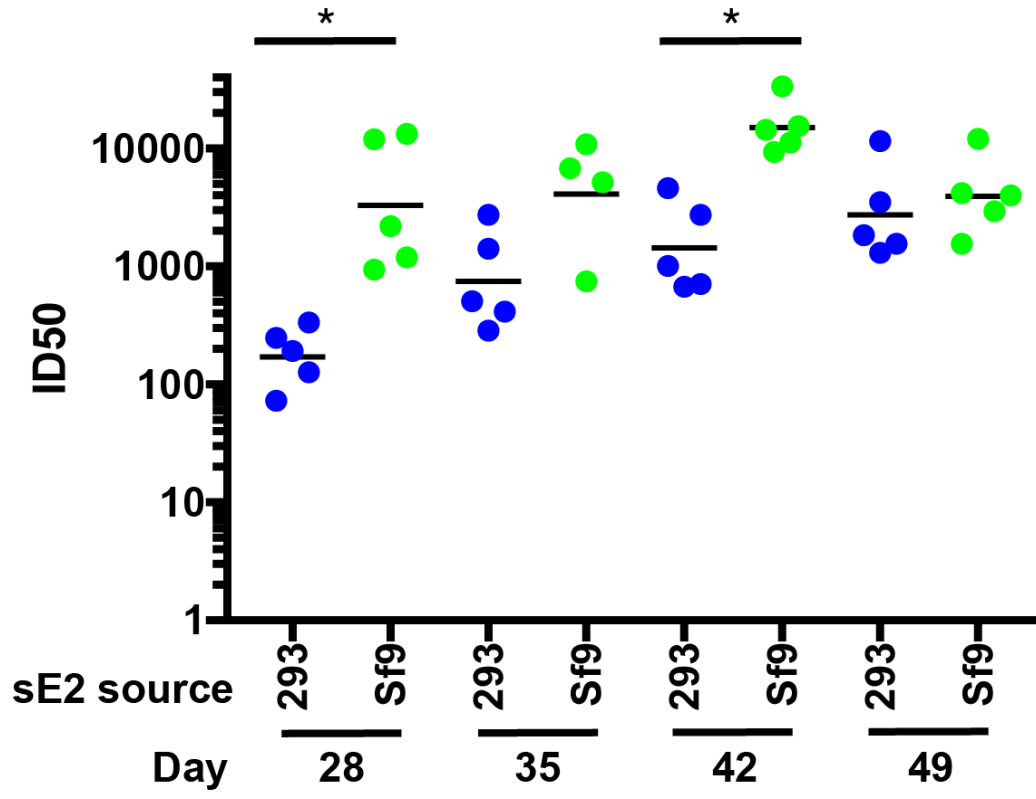
756 **Figure 7.**

757

758

759 Figure 8.

760



761

762

Figure 9.

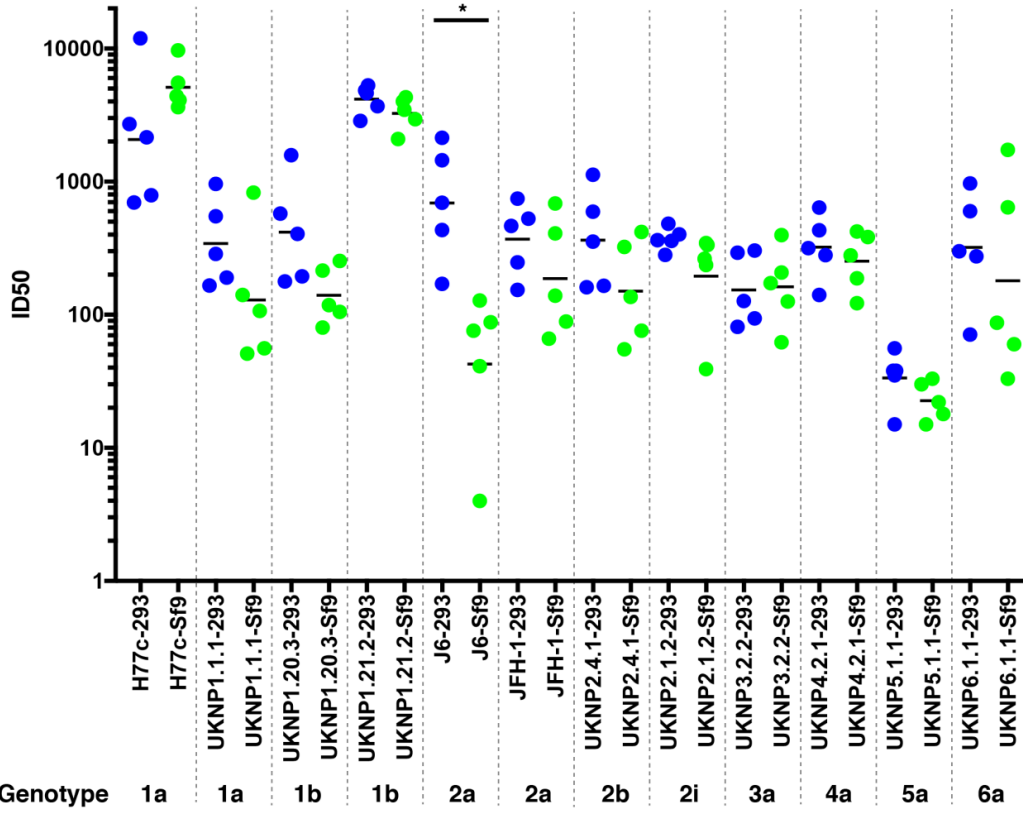
763
764

Table 1. Analytical gradient

Time	(mL/min)	% B (0.1 % FA in ACN)	Divert Valve	MS Data Collection
0	0.25	1	Waste	No
2	0.25	1	MS	Yes
6	0.25	10	MS	Yes
70	0.25	35	Waste	No
72	0.25	90	Waste	No
77	0.25	90	Waste	No
79	0.25	1	Waste	No
81	0.25	1	Waste	No
83.5	0.25	10	Waste	No
91.5	0.25	45	Waste	No
93	0.25	90	Waste	No
99	0.25	90	Waste	No
101	0.25	1	Waste	No
115	0.25	1	Waste	No

765

766 **Table 2.** Calculated E2 percent surface occlusion by most abundant N-glycans from HEK293
767 and Sf9 expression systems modeled onto the E2 core structure.

Probe Radius (Å)	HEK293	Sf9
1.4	20%	21%
5	49%	43%
10	64%	55%

768

769

770 **Table 3.** Affinities of HEK293 sE2 and Sf9 sE2 for CD81 and HMAbs
 771

Ligand	HEK293 sE2		Sf9 sE2	
	K_D (nM)	R^2	K_D (nM)	R^2
CD81	510 ± 22	0.997	440 ± 38	0.984
HC84.26 ^a	1.8 ± 0.5	0.965	2.7 ± 0.8	0.965
HC84.24 ^a	1.9 ± 0.3	0.962	1200 ± 29	0.980
CBH-4B ^b	11 ± 1.7	0.971	120 ± 11	0.926
CBH-4G ^b	120 ± 33	0.949	no binding	–
HCV1 ^c	36 ± 3.0	0.985	9.3 ± 2.0	0.946
HC33.1 ^c	50 ± 9.9	0.979	47 ± 9.9	0.927
HC-1 ^d	65 ± 1.0	0.980	69 ± 6.5	0.993
HC-11 ^d	7.0 ± 1.3	0.975	25 ± 4.4	0.974

772 ^aSpecific for antigenic domain D. ^bSpecific for antigenic domain A.

773 ^cSpecific for antigenic domain E. ^dSpecific for antigenic domain B.

774

775 **REFERENCES**

- 776 1. <http://www.who.int/mediacentre/factsheets/fs164/en>
- 777 2. Liang TJ, Ghany MG. 2013. Current and future therapies for hepatitis C virus infection.
778 *N Engl J Med* **368**:1907-1917.
- 779 3. González-Grande R, Jiménez-Pérez M, González Arjona C, Mostazo Torres J. 2016.
780 New approaches in the treatment of hepatitis C. *World J Gastroenterol* **22**:1421-1423.
- 781 4. Cox A. 2015. Global control of hepatitis C virus. *Science* **349**:790-791.
- 782 5. Osburn WO, Snider AE, Wells BL, Latanich R, Bailey JR, Thomas DL, Cox AL, Ray
783 SC. 2014. Clearance of hepatitis C infection is associated with the early appearance of
784 broad neutralizing antibody responses. *Hepatology* **59**:2140-2151.
- 785 6. Pestka JM, Zeisel MB, Bläser E, Schürmann P, Bartosch B, Cosset FL, Patel AH,
786 Meisel H, Baumert J, Viazov S, Rispeter K, Blum HE, Roggendorf M, Baumert TF.
787 2007. Rapid induction of virus-neutralizing antibodies and viral clearance in a
788 single-source outbreak of hepatitis C. *Proc Natl Acad Sci USA* **104**:6025-6030.
- 789 7. Pierce BG, Keck ZY, Lau P, Fauvelle C, Gowthaman R, Baumert TF, Fuerst TR,
790 Mariuzza RA, Fong SK. 2016. Global mapping of antibody recognition of the
791 hepatitis C virus E2 glycoprotein: Implications for vaccine design. *Proc Natl Acad Sci*
792 *USA* **113**:E6946-E6954.
- 793 8. Gopal R, Jackson K, Tzarum N, Kong L, Ettenger A, Guest J, Pfaff JM, Barnes T,
794 Honda A, Giang E, Davidson E, Wilson IA, Doranz BJ, Law M. 2017. Probing the
795 antigenicity of hepatitis C virus envelope glycoprotein complex by high-throughput
796 mutagenesis. *PLoS Pathog* **13**:e1006735.
- 797 9. Bukh J, Engle RE, Faulk K, Wang RY, Farci P, Alter HJ, Purcell RH. 2015.
798 Immunoglobulin with high-titer in vitro cross-neutralizing hepatitis C virus antibodies
799 passively protects chimpanzees from homologous, but not heterologous, challenge. *J*
800 *Viro* **89**: 9128-9132.
- 801 10. Morin TJ, Broering TJ, Leav BA, Blair BM, Rowley KJ, Boucher EN, Wang Y,
802 Cheslock PS, Knauber M, Olsen DB, Ludmerer SW, Szabo G, Finberg RW, Purcell RH,
803 Lanford RE, Ambrosino DM, Molrine DC, Babcock GJ. 2012. Human monoclonal
804 antibody HCV1 effectively prevents and treats HCV infection in chimpanzees. *PLoS*
805 *Pathog* **8**:e1002895.
- 806 11. Weiner AJ, Geysen HM, Christopherson C, Hall JE, Mason TJ, Saracco G, Bonino F,
807 Crawford K, Marion CD, Crawford KA, et al. 1992. Evidence for immune selection of
808 hepatitis C virus (HCV) putative envelope glycoprotein variants: potential role in
809 chronic HCV infections. *Proc Natl Acad Sci USA* **89**:3468-3472.
- 810 12. Goffard A, Callens N, Bartosch B, Wychowski C, Cosset FL, Montpellier C, Dubuisson
811 J. 2005. Role of N-linked glycans in the functions of hepatitis C virus envelope
812 glycoproteins. *J Virol* **79**:8400-8409.
- 813 13. Falkowska E, Kajumo F, Garcia E, Reinus J, Dragic T. 2007. Hepatitis C virus envelope
814 glycoprotein E2 glycans modulate entry, CD81 binding, and neutralization. *J Virol*
815 **81**:8072-8079.
- 816 14. Helle F, Goffard A, Morel V, Duverlie G, McKeating J, Keck ZY, Fong S, Penin F,
817 Dubuisson J, Voisset C. 2007. The neutralizing activity of anti-hepatitis C virus

- 818 antibodies is modulated by specific glycans on the E2 envelope protein. *J Virol*
819 **81**:8101-8111.
- 820 15. Helle F, Vieyres G, Elkrief L, Popescu CI, Wychowski C, Descamps V, Castelain S,
821 Roingeard P, Duverlie G, Dubuisson J. 2010. Role of N-linked glycans in the functions
822 of hepatitis C virus envelope proteins incorporated into infectious virions. *J Virol*
823 **84**:11905-11915.
- 824 16. Lavie M, Hanouille X, Dubuisson J. 2018. Glycan shielding and modulation of hepatitis
825 C virus neutralizing antibodies. *Front Immunol* **9**:910.
- 826 17. Julien J-P, Lee PS, Wilson IA. 2012. Structural insights into key sites of vulnerability
827 on HIV-1 Env and influenza HA. *Immunol Rev* **250**:180-198.
- 828 18. Ingale J, Tran K, Kong L, Dey B, McKee K, Schief W, Kwong PD, Mascola JR, Wyatt
829 RT. 2014. Hyperglycosylated stable core immunogens designed to present the CD4
830 binding site are preferentially recognized by broadly neutralizing antibodies. *J Virol*
831 **88**:14002-14016.
- 832 19. Pantophlet R, Wilson IA, Burton DR. 2003. Hyperglycosylated mutants of human
833 immunodeficiency virus (HIV) type 1 monomeric gp120 as novel antigens for HIV
834 vaccine design. *J Virol* **77**:5889-5901.
- 835 20. Ringe RP, Ozorowski G, Rantalainen K, Struwe WB, Matthews K, Torres JL, Yasmeen
836 A, Cottrell CA, Ketas TJ, LaBranche CC, Montefiori DC, Cupo A, Crispin M, Wilson
837 IA, Ward AB, Sanders RW, Klasse PJ, Moore JP. 2017. Reducing V3 antigenicity and
838 immunogenicity on soluble, native-like HIV-1 Env SOSIP trimers. *J Virol* **91**:pii:
839 e00677-17.
- 840 21. Wanzeck K, Boyd KL, McCullers JA. 2011. Glycan shielding of the influenza virus
841 hemagglutinin contributes to immunopathology in mice. *Am J Respir Crit Care Med*,
842 **183**:767-773.
- 843 22. Wei CJ, Boyington JC, Dai K, Houser KV, Pearce MB, Kong WP, Yang ZY, Tumpey
844 TM, Nabel GJ. 2010. Cross-neutralization of 1918 and 2009 influenza viruses: role of
845 glycans in viral evolution and vaccine design. *Sci Transl Med* **2**:24ra21.
- 846 23. Behrens AJ, Vasiljevic S, Pritchard LK, Harvey DJ, Andev RS, Krumm SA, Struwe
847 WB, Cupo A, Kumar A, Zitzmann N, Seabright GE, Kramer HB, Spencer DI, Royle L,
848 Lee JH, Klasse PJ, Burton DR, Wilson IA, Ward AB, Sanders RW, Moore JP, Doores
849 KJ, Crispin M. 2016. Composition and antigenic effects of individual glycan sites of a
850 trimeric HIV-1 envelope glycoprotein. *Cell Rep* **14**:2695-2706.
- 851 24. Liang Y, Guttman M, Williams JA, Verkerke H, Alvarado D, Hu SL, Lee KK. 2016.
852 Changes in structure and antigenicity of HIV-1 Env trimers resulting from removal of a
853 conserved CD4 binding site-proximal glycan. *J Virol* **90**:9224-9236.
- 854 25. McGuire AT, Hoot S, Dreyer AM, Lippy A, Stuart A, Cohen KW, Jardine J, Menis S,
855 Scheid JF, West AP, Schief WR, Stamatatos L. 2013. Engineering HIV envelope
856 protein to activate germline B cell receptors of broadly neutralizing anti-CD4 binding
857 site antibodies. *J Exp Med* **210**:655-663.
- 858 26. Medina-Ramírez M, Garcés F, Escolano A, Skog P, de Taeye SW, Del Moral-Sánchez I,
859 McGuire AT, Yasmeen A, Behrens AJ, Ozorowski G, van den Kerkhof TLGM, Freund
860 NT, Dosenovic P, Hua Y, Gitlin AD, Cupo A, van der Woude P, Golabek M, Slieden K,
861 Blane T, Kootstra N, van Breemen MJ, Pritchard LK, Stanfield RL, Crispin M, Ward

- 862 AB, Stamatatos L, Klasse PJ, Moore JP, Nemazee D, Nussenzweig MC, Wilson IA,
863 Sanders RW. 2017. Design and crystal structure of a native-like HIV-1 envelope trimer
864 that engages multiple broadly neutralizing antibody precursors in vivo. *J Exp Med*
865 **214**:2573-2590.
- 866 27. Medina RA, Stertz S, Manicassamy B, Zimmermann P, Sun X, Albrecht RA,
867 Uusi-Kerttula H, Zagordi O, Belshe RB, Frey SE, Tumpey TM, García-Sastre A. 2013.
868 Glycosylations in the globular head of the hemagglutinin protein modulate the
869 virulence and antigenic properties of the H1N1 influenza viruses. *Sci Transl Med*
870 **5**:187ra170.
- 871 28. Zhou T, Doria-Rose NA, Cheng C, Stewart-Jones GBE, Chuang GY, Chambers M,
872 Druz A, Geng H, McKee K, Kwon YD, O'Dell S, Sastry M, Schmidt SD, Xu K, Chen
873 L, Chen RE, Louder MK, Pancera M, Wanninger TG, Zhang B, Zheng A, Farney
874 SK, Foulds KE, Georgiev IS, Joyce MG, Lemmin T, Narpala S, Rawi R, Soto C, Todd
875 JP, Shen CH, Tsybovsky Y, Yang Y, Zhao P, Haynes BF, Stamatatos L, Tiemeyer M,
876 Wells L, Scorpio DG, Shapiro L, McDermott AB, Mascola JR, Kwong PD. 2017.
877 Quantification of the impact of the HIV-1 glycan shield on antibody elicitation. *Cell*
878 *Rep* **19**:719-732.
- 879 29. Grzyb K, Czarnota A, Brzozowska A, Cieślik A, Rąbalski Ł, Tyborowska J,
880 Bieńkowska-Szewczyk K. 2016. Immunogenicity and functional characterization of
881 *Leishmania*-derived hepatitis C virus envelope glycoprotein complex. *Sci Rep*
882 **6**:30627.
- 883 30. Kong L, Sheppard NC, Stewart-Jones GB, Robson CL, Chen H, Xu X, Krashias G,
884 Bonomelli C, Scanlan CN, Kwong PD, Jeffs SA, Jones IM, Sattentau QJ. 2010.
885 Expression-system-dependent modulation of HIV-1 envelope glycoprotein antigenicity
886 and immunogenicity. *J Mol Biol* **403**:131-147.
- 887 31. Li D, von Schaeuwen M, Wang X, Tao W, Zhang Y, Li L, Heller B, Hrebikova G, Deng
888 Q, Ploss A, Zhong J, Huang Z. 2016. Altered glycosylation patterns increase
889 immunogenicity of a subunit hepatitis C virus vaccine, inducing neutralizing antibodies
890 which confer protection in mice. *J Virol* **90**:10486-10498.
- 891 32. Raska M, Takahashi K, Czernekova L, Zachova K, Hall S, Moldoveanu Z, Elliott MC,
892 Wilson L, Brown R, Jancova D, Barnes S, Vrbkova J, Tomana M, Smith PD, Mestecky
893 J, Renfrow MB, Novak J. 2010. Glycosylation patterns of HIV-1 gp120 depend on the
894 type of expressing cells and affect antibody recognition. *J Biol Chem* **285**:
895 20860-20869.
- 896 33. Wang CC, Chen JR, Tseng YC, Hsu CH, Hung YF, Chen SW, Chen CM, Khoo KH,
897 Cheng TJ, Cheng YS, Jan JT, Wu CY, Ma C, Wong CH. 2009. Glycans on influenza
898 hemagglutinin affect receptor binding and immune response. *Proc Natl Acad Sci USA*
899 **106**:18137-18142.
- 900 34. Labonte JW, Adolf-Bryfogle J, Schief WR, Gray JJ. 2017. Residue-centric modeling
901 and design of saccharide and glycoconjugate structures. *J Comput Chem* **38**: 276-287.
- 902 35. Kong L, Giang E, Nieusma T, Kadam RU, Cogburn KE, Hua Y, Dai X, Stanfield RL,
903 Burton DR, Ward AB, Wilson IA, Law M. 2013. Hepatitis C virus E2 envelope
904 glycoprotein core structure. *Science* **342**:1090-1094.

- 905 36. Kleiger G, Saha A, Lewis S, Kuhlman B, Deshaies RJ. 2009. Rapid E2-E3 assembly
906 and disassembly enable processive ubiquitylation of cullin-RING ubiquitin ligase
907 substrates. *Cell* **139**:957-968.
- 908 37. Broering TJ, Garrity KA, Boatright NK, Sloan SE, Sandor F, Thomas WD Jr, Szabo G,
909 Finberg RW, Ambrosino DM, Babcock GJ. 2009. Identification and characterization of
910 broadly neutralizing human monoclonal antibodies directed against the E2 envelope
911 glycoprotein of hepatitis C virus. *J Virol* **83**:12473-12482.
- 912 38. Keck ZY, Xia J, Wang Y, Wang W, Krey T, Prentoe J, Carlsen T, Li AY, Patel AH,
913 Lemon SM, Bukh J, Rey FA, Fong SK. 2012. Human monoclonal antibodies to a
914 novel cluster of conformational epitopes on HCV E2 with resistance to neutralization
915 escape in a genotype 2a isolate. *PLoS Pathog* **8**:e1002653.
- 916 39. Tarr AW, Urbanowicz RA, Hamed MR, Albecka A, McClure CP, Brown RJ, Irving
917 WL, Dubuisson J, Ball JK. 2011. Hepatitis C patient-derived glycoproteins exhibit
918 marked differences in susceptibility to serum neutralizing antibodies: genetic subtype
919 defines antigenic but not neutralization serotype. *J Virol* **85**:4246-4257.
- 920 40. Urbanowicz RA, McClure CP, Brown RJ, Tsoleridis T, Persson MA, Krey T, Irving
921 WL, Ball JK, Tarr AW. 2015. A diverse panel of hepatitis C virus glycoproteins for use
922 in vaccine research reveals extremes of monoclonal antibody neutralization resistance.
923 *J Virol* **90**:3288-3301.
- 924 41. Urbanowicz RA, McClure CP, King B, Mason CP, Ball JK, Tarr AW. 2016. Novel
925 functional hepatitis C virus glycoprotein isolates identified using an optimized viral
926 pseudotype entry assay. *J Gen Virol* **97**:2265-2279.
- 927 42. Shi X, Jarvis DL. 2007. Protein N-glycosylation in the baculovirus-insect cell system.
928 *Curr Drug Targets* **8**:1116-1125.
- 929 43. Walski T, De Schutter K, Van Damme EJM, Smagghe G. 2017. Diversity and functions
930 of protein glycosylation in insects. *Insect Biochem Mol Biol* **83**:21-34.
- 931 44. Kato N, Sekiya H, Ootsuyama Y, Nakazawa T, Hijikata M, Ohkoshi S, Shimotohno K.
932 1993. Humoral immune response to hypervariable region 1 of the putative envelope
933 glycoprotein (gp70) of hepatitis C virus. *J Virol* **67**:3923-3930.
- 934 45. Farci P, Shimoda A, Wong D, Cabezon T, De Gioannis D, Strazzera A, Shimizu Y,
935 Shapiro M, Alter HJ, Purcell RH. 1996. Prevention of hepatitis C virus infection in
936 chimpanzees by hyperimmune serum against the hypervariable region 1 of the
937 envelope 2 protein. *Proc Natl Acad Sci USA* **93**:15394-15399.
- 938 46. von Hahn T, Yoon JC, Alter H, Rice CM, Rehermann B, Balfe P, McKeating JA. 2007.
939 Hepatitis C virus continuously escapes from neutralizing antibody and T-cell responses
940 during chronic infection in vivo. *Gastroenterology* **132**:667-678.
- 941 47. Dowd KA, Netski DM, Wang XH, Cox AL, Ray SC. 2009. Selection pressure from
942 neutralizing antibodies drives sequence evolution during acute infection with hepatitis
943 C virus. *Gastroenterology* **136**:2377-2386.
- 944 48. Vieyres G, Thomas X, Descamps V, Duverlie G, Patel AH, Dubuisson J. 2010.
945 Characterization of the envelope glycoproteins associated with infectious hepatitis C
946 virus. *J Virol* **84**:10159-10168.

- 947 49. Jacob RE, Perdivara I, Przybylski M, Tomer KB. 2008. Mass spectrometric
948 characterization of glycosylation of hepatitis C virus E2 envelope glycoprotein reveals
949 extended microheterogeneity of N-glycans. *J Am Soc Mass Spectrom* **19**:428-444.
- 950 50. Banerjee K, Andjelic S, Klasse PJ, Kang Y, Sanders RW, Michael E, Durso RJ, Ketas
951 TJ, Olson WC, Moore JP. 2009. Enzymatic removal of mannose moieties can increase
952 the immune response to HIV-1 gp120 in vivo. *Virology* **389**:108-121.
- 953 51. Ciabattini A, Pettini E, Fiorino F, Pastore G, Andersen P, Pozzi G, Medaglini D. 2016.
954 Modulation of primary immune response by different vaccine adjuvants. *Front*
955 *Immunol* **7**:427.
- 956 52. Prentoe J, Velázquez-Moctezuma R, Fong SK, Law M, Bukh J. 2016. Hypervariable
957 region 1 shielding of hepatitis C virus is a main contributor to genotypic differences in
958 neutralization sensitivity. *Hepatology* **64**:1881-1892.
- 959 53. Bailey JR, Wasilewski LN, Snider AE, El-Diwany R, Osburn WO, Keck Z, Fong SK,
960 Ray SC. 2015. Naturally selected hepatitis C virus polymorphisms confer broad
961 neutralizing antibody resistance. *J Clin Invest* **125**:437-447.
- 962 54. Medina-Ramírez M, Sanders RW, Sattentau QJ. 2017. Stabilized HIV-1 envelope
963 glycoprotein trimers for vaccine use. *Curr Opin HIV AIDS* **12**:241-249.
- 964 55. Bhattacharyya S, Rajan RE, Swarupa Y, Rathore U, Verma A, Udaykumar R,
965 Varadarajan R. 2010. Design of a non-glycosylated outer domain-derived HIV-1 gp120
966 immunogen that binds to CD4 and induces neutralizing antibodies. *J Biol Chem*
967 **285**:27100-27110.
- 968 56. Kumar R, Tuen M, Li H, Tse DB, Hioe CE. 2011. Improving immunogenicity of
969 HIV-1 envelope gp120 by glycan removal and immune complex formation. *Vaccine*
970 **29**:9064-9074.
971